Agricultural Water Management 111 (2012) 87–104

Contents lists available at SciVerse ScienceDirect

Agricultural Water Management

journal homepage: www.elsevier.com/locate/agwat

Two-dimensional modeling of water and nitrogen fate from sweet sorghum irrigated with fresh and blended saline waters

T.B. Ramos[a,*], J. Šimůnek[b], M.C. Gonçalves[a,c], J.C. Martins[c], A. Prazeres[c], L.S. Pereira[a]

[a] CEER-Biosystems Engineering, Institute of Agronomy, Technical University of Lisbon, Tapada da Ajuda, 1349-017, Lisbon, Portugal
[b] Department of Environmental Sciences, University of California, Riverside, CA, 92521, USA
[c] Estação Agronómica Nacional, INIA, Instituto Nacional de Recursos Biológicos, Quinta do Marquês, Av. República, 2784-505, Oeiras, Portugal

ARTICLE INFO

Article history:
Received 21 October 2011
Received in revised form 18 May 2012
Accepted 21 May 2012
Available online 8 June 2012

Keywords:
HYDRUS-2D
Saline irrigation water
Nitrates leaching
Sorghum yields

ABSTRACT

The need for reducing irrigation water demand and non-point source pollution all across Europe has made sweet sorghum [*Sorghum bicolor* (L.) Moench], due to its lower water and nutrient requirements, an interesting alternative to other traditional summer crops in European Mediterranean regions. HYDRUS-2D was used to model the fate of nitrogen in a plot planted with sweet sorghum grown under Mediterranean conditions between 2007 and 2010, while considering drip irrigation scenarios with different levels of nitrogen and salty waters. HYDRUS-2D simulated water contents, EC_{sw}, and $N{-}NH_4^+$ and $N{-}NO_3^-$ concentrations continuously for the entire duration of the field experiment, while producing RMSE between simulated and measured data of 0.030 $cm^3\,cm^{-3}$, 1.764 $dS\,m^{-1}$, 0.042 $mmol_c\,L^{-1}$, and 3.078 $mmol_c\,L^{-1}$, respectively. Estimates for sweet sorghum water requirements varied between 360 and 457 mm depending upon the crop season and the irrigation treatment. Sweet sorghum proved to be tolerant to saline waters if applied only during one crop season. However, the continuous use of saline waters for more than one crop season led to soil salinization, and to root water uptake reductions due to the increasing salinity stress. The relation found between $N{-}NO_3^-$ uptake and dry biomass yield ($R^2 = 0.71$) showed that nitrogen needs were smaller than the uptakes estimated for the scenario with the highest levels of nitrogen application. The movement of N out of the root zone was dependent on the amount of water flowing through the root zone, the amount of N applied, the form of N in the fertilizer, and the timing and number of fertigation events. The simulations with HYDRUS-2D were useful to understand the best strategies toward increasing nutrient uptake and reducing nutrient leaching. In this sense, $N{-}NO_3^-$ uptakes were higher when fertigation events were more numerous and the amounts applied per event smaller.

1. Introduction

Non-point source pollution is among the most important and widespread environmental problems in European Mediterranean agricultural regions. Farmers usually apply high rates of water and nitrogen fertilizer to insure that crop needs are fulfilled, while producing inefficient water and nitrogen use, and increasing leaching potential of nutrients into the groundwater.

The European Commission implemented the Council Directive 91/676/EEC in 1991, also referred to as the Nitrates Directive, which imposed upon EU-Member States the establishment of various action programs for reducing water contamination caused or induced by agricultural sources. However, 20 years later many European regions with higher agriculture intensity continue registering high nitrate concentrations in a significant number of groundwater monitoring stations. In particular, many monitoring stations in the European Mediterranean Member States showed relatively high values throughout 2004–2007. Nitrate vulnerable zones covered 3.7% of Portugal, 6.8% of Cyprus, 12.6% of Spain and Italy, 24.2% of Greece, and 100% of Malta's territories (European Commission, 2010a,b).

In these water-scarce European Mediterranean regions, the use of crops with lower water and nutrient needs has recently been considered to be an adequate alternative to traditional crops such as corn, in order to reduce nutrient loads into the groundwater (Barbanti et al., 2006). Sweet sorghum (*Sorghum bicolor* (L.) Moench) was regarded among the most interesting annual crops to be grown in these environmentally stressed areas (Almodares and Hadi, 2009; Vasilakoglou et al., 2011). Sweet sorghum is a drought resistant crop with relatively low water requirements and high water-use efficiency (Mastrorilli et al., 1995, 1999; Steduto et al., 1997; Katerji et al., 2008), and is moderately tolerant to

* Corresponding author. Tel.: +351 214403500; fax: +351 214416011.
E-mail address: tiago_ramos@netcabo.pt (T.B. Ramos).

0378-3774/$ – see front matter © 2012 Elsevier B.V. All rights reserved.
http://dx.doi.org/10.1016/j.agwat.2012.05.007

salinity (Maas, 1990; Hoffman and Shalhevet, 2007). Sweet sorghum is furthermore an important alternative source for renewable energy because of its ability to store large quantities of non-structural carbohydrates (sucrose, glucose, and fructose) in its stems that can be converted into fuel ethanol (Prasad et al., 2007; Zhao et al., 2009; Almodares and Hadi, 2009).

A large number of analytical and numerical modeling tools are available to evaluate the effects of different agricultural practices on nitrogen leaching, nutrient uptake, and crop yield (e.g., Johnsson et al., 1987; Hutson and Wagenet, 1991; Ma et al., 2001; Šimůnek et al., 2008; Doltra and Muñoz, 2010). Simulation models can rapidly perform a long-term analysis of the effects of introducing new crops and/or new agricultural practices in nitrate vulnerable zones, and help develop action programs to minimize nutrient loads into groundwater as required by the Nitrates Directive.

Some of those physical-based models have been calibrated and/or validated to simulate water movement (Fernando, 1993; Cameira et al., 2005), nutrient transport (Cameira et al., 2003, 2007), soil salinity distribution (Gonçalves et al., 2006; Ramos et al., 2011), and runoff and soil erosion (Fontes et al., 1992) in different regions of Portugal. Semi-empirical water balance models have also been developed to improve irrigation scheduling and reduce water losses (Pereira et al., 1995; Rosa et al., 2012). However, these approaches have been only one-dimensional and neglected water and solute fluxes, and pressure head and concentration gradients in the horizontal direction. Additionally, one-dimensional models fail to adequately simulate micro-irrigation systems (such as drip emitters, drip tape, and micro-sprinklers), which can efficiently apply water and nutrients in the right amounts and precise locations throughout a field (Gärdenäs et al., 2005). Since drip irrigation is often used in Portugal it seems only adequate to find modeling approaches that are more suitable to represent complex physical and chemical processes that take place in the soil profile under this irrigation system.

The HYDRUS (2D/3D) software package (Šimůnek et al., 2006, 2008) is the state-of-the-art model for simulating water, heat, and solute movement in two- and three-dimensional variably saturated porous media that can become a valuable tool for establishing sound agricultural practices in European Mediterranean agricultural regions. The model has been extensively used for simulating the fate of nutrients in soils by evaluating and comparing micro-irrigation and fertigation strategies for different crops (Cote et al., 2003; Gärdenäs et al., 2005; Hanson et al., 2006; Ajdary et al., 2007; Crevoisier et al., 2008). It has also been used for a wide range of applications of interest for water scarce regions, such as improving irrigation management with poor quality waters (Gonçalves et al., 2006; Hanson et al., 2008; Roberts et al., 2008, 2009; Ramos et al., 2011). Furthermore, HYDRUS-2D (a two-dimensional module of HYDRUS (2D/3D)) results are often used as a reference for developing or validating new simulation models (Mmolawa and Or, 2003; Doltra and Muñoz, 2010; Mailhol et al., 2011).

The main objective of this study was to use the HYDRUS-2D software package to model nitrogen fate in a plot with sweet sorghum grown under Mediterranean conditions while considering different drip fertigation and water quality scenarios. From 2007 to 2010 (i.e., during three crop seasons), sweet sorghum was subjected to the application of different amounts of nitrogen, different fertigation events, and to irrigation with waters of different quality. Field data were used to calibrate and validate HYDRUS-2D for predicting (i) soil water contents and fluxes, (ii) the electrical conductivity of the soil solution (EC_{sw}), (iii) water uptake reductions due to the use of saline waters, and (iv) $N—NH_4^+$ and $N—NO_3^-$ concentrations in the soil and leaching. Water and nutrient balances were calculated based on HYDRUS-2D predictions for three crop seasons and for the entire simulation period. The modeling approach helped us understand the best irrigation and fertigation management practices to be adopted in future practical applications for increasing nutrient uptake and reducing nutrient leaching.

Table 1
Main physical and chemical soil characteristics.

Depth (cm)	Alvalade		
	0–30	30–75	75–100
Coarse sand, 2000–200 μm (%)	8.3	6.5	5.8
Fine sand, 200–20 μm (%)	52.4	46.2	42.0
Silt, 20–2 μm (%)	26.3	29.3	27.6
Clay, <2 μm (%)	13.0	18.0	24.6
Texture	Loam	Silty loam	Loam
Bulk density ($g\,cm^{-3}$)	1.49	1.51	1.61
pH (H_2O)	7.27	7.23	7.21
Organic matter (%)	2.30	2.26	1.66
Soil initial conditions:			
Water content ($cm^3\,cm^{-3}$)	0.18	0.18	0.18
EC_{sw} ($dS\,m^{-1}$)	2.17	2.99	4.68
$N—NH_4^+$ ($mmol_c\,L^{-1}$)	0.01	0.01	0.01
$N—NO_3^-$ ($mmol_c\,L^{-1}$)	0.31	0.47	1.43
van Genuchten–Mualem parameters:			
θ_r ($cm^3\,cm^{-3}$)	0.050	0.108	0.000
θ_s ($cm^3\,cm^{-3}$)	0.380	0.380	0.375
α (cm^{-1})	0.027	0.115	0.045
η (–)	1.21	1.19	1.17
ℓ (–)	−4.41	−5.37	−6.48
K_s ($cm\,d^{-1}$)	16.6	84.4	21.0
Solute transport parameters:			
ε_L (cm)	25.8	25.8	12.2

EC_{sw}, electrical conductivity of the soil solution; θ_r, residual water content; θ_s, saturated water content; α and η, are empirical shape parameters; ℓ, pore connectivity/tortuosity parameter; K_s, saturated hydraulic conductivity; ε_L, longitudinal dispersivity.

2. Materials and methods

2.1. Experimental setup and measurements

The field experiment was conducted at the Alvalade Experimental Station (37°56′48″N and 8°23′40″W), southern Portugal, from May 2007 to April 2010. The climate in the region is dry, sub-humid, with hot dry summers and mild winters with irregular rainfall. Rainfall was 371, 299, and 676 mm in 2007/2008, 2008/2009, and 2009/2010, respectively, with 91, 63, and 35 mm of rain during the corresponding crop growth seasons. The soil was classified as a Eutric Fluvisol (FAO, 2006). The soil's main physical and chemical properties are presented in Table 1. Field and laboratory methodologies used for characterizing the soil profile were extensively described by Ramos et al. (2011).

The field experiment involved irrigation of sweet sorghum (*S. bicolor* (L.) Moench var. *saccharatum* (L.) Mohlenbr) with synthetic saline waters blended with fresh irrigation waters and waters with nitrogen (NH_4NO_3) during three crop seasons. The crop hybrid selected for this experiment was the sweet sorghum "Madhura", developed in India. Sweet sorghum was sown on May 18, 2007, May 15, 2008, and May 15, 2009. The row spacing used was 0.75 m and the distance between plants was 0.15 m. Irrigation started on June 1, 2007 (15 days after sowing, or DAS), June 13, 2008 (30 DAS), and June 3, 2009 (20 DAS). The total amount of water applied was 425, 522, and 546 mm in 2007, 2008, and 2009, respectively.

The drip irrigation system was used to mix and deliver synthetic saline irrigation waters, fresh irrigation waters, and fertilizer (NH_4NO_3) to the experimental plots following the irrigation scheme documented in Ramos et al. (2009, 2011). This system consisted of three drip lines connected together in order to form a triple joint lateral placed along each sweet sorghum line (Fig. 1). The first of the laterals was connected to the salt stock solution

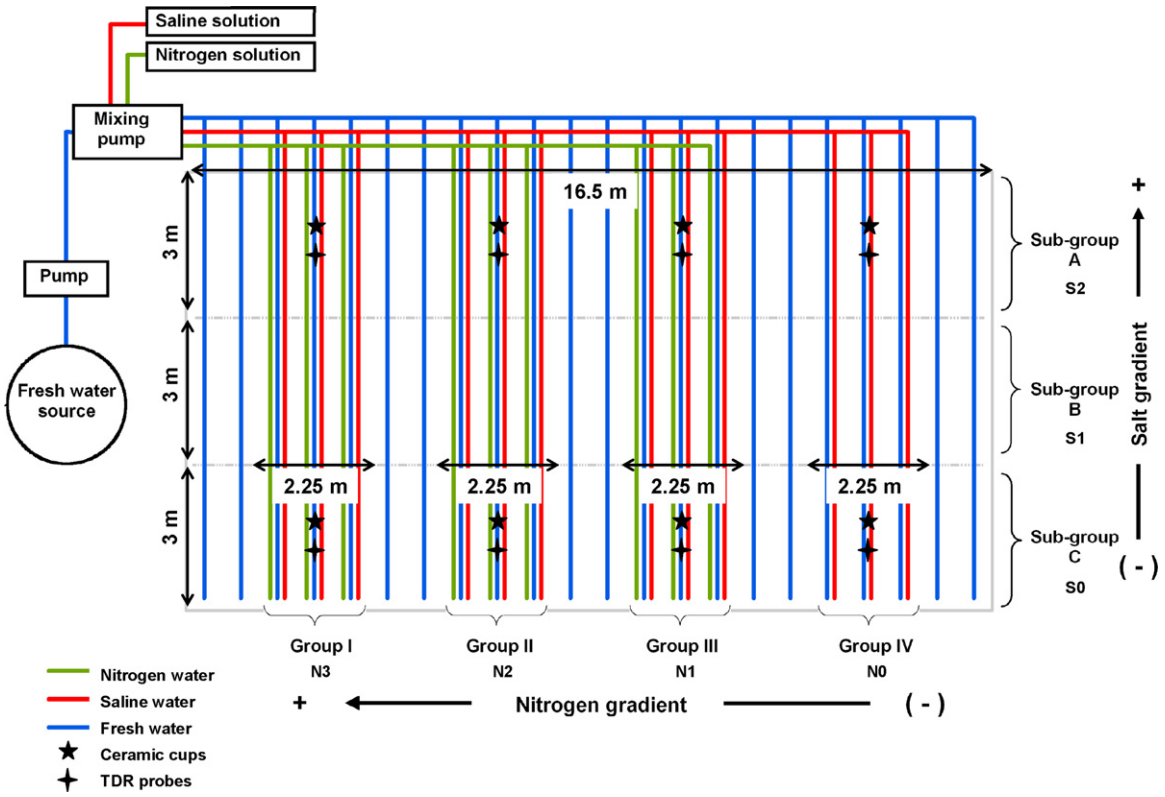

Fig. 1. Layout of the triple emitter source design (adapted from Ramos et al., 2009). The salt gradient decreases from sub-group A to C and the fertilizer gradient decreases from group I to IV.

Table 2
Discharge rates of the laterals applying salt (Na^+), nitrogen (N) and fresh water (W) in each experimental plot. There is an overall constant cumulative discharge at each dripping point of 18 L h^{-1} m^{-1} (Ramos et al., 2009).

Treatment	Application rates (L h^{-1} m^{-1})											
	Group I			Group II			Group III			Group IV		
	Na^+	N	W	Na^+	N	W	Na^+	N	W	Na^+	N	W
A	12	6	0	12	4	2	12	2	4	12	0	6
B	6	6	6	6	4	8	6	2	10	6	0	12
C	0	6	12	0	4	14	0	2	16	0	0	18

(NaCl), while the second one was connected to the nitrogen reservoir. The third lateral delivered fresh water and was used to obtain a constant water application rate for each dripping point along the triple joint lateral (the drip discharge of 18 L h^{-1} m^{-1}; which represents 24 mm h^{-1} considering an area for each dripping point of 100 cm × 75 cm). Gradients of applied salt (Na^+) and nitrogen (N) concentrations were then produced by placing different emitters in each dripping point along the corresponding laterals and

Table 3
Waters blended in each experimental plot during the three crop seasons.

Sub-group	Irrigation water	Water applied (mm)											
		Group I			Group II			Group III			Group IV		
		2007	(N3) 2008	2009	2007	(N2) 2008	2009	2007	(N1) 2008	2009	2007	(N0) 2008	2009
A (S2)	Saline water	228.0	184.0	316.0	228.0	184.0	316.0	228.0	184.0	316.0	228.0	184.0	316.0
	Water + NH_4NO_3	19.3	30.0	20.0	12.9	20.0	13.3	6.4	10.0	6.7	0.0	0.0	0.0
	Fresh water	177.7	308.0	210.0	184.1	318.0	216.7	190.6	328.0	223.3	197.0	338.0	230.0
B (S1)	Saline water	114.0	92.0	158.0	114.0	92.0	158.0	114.0	92.0	158.0	114.0	92.0	158.0
	Water + NH_4NO_3	19.3	30.0	20.0	12.9	20.0	13.3	6.4	10.0	6.7	0.0	0.0	0.0
	Fresh water	291.7	400.0	368.0	298.1	410.0	374.7	304.6	420.0	381.3	311.0	430.0	388.0
C (S0)	Saline water	0.0	0.0	0.0	0.0	0.0	0.0	0.0	0.0	0.0	0.0	0.0	0.0
	Water + NH_4NO_3	19.3	30.0	20.0	12.9	20.0	13.3	6.4	10.0	6.7	0.0	0.0	0.0
	Fresh water	405.7	492.0	526.0	412.1	502.0	532.7	418.6	512.0	539.3	425.0	522.0	546.0

N3, N2, N1, N0, nitrogen gradient; S2, S1, S0, salinity gradient.

Table 4
Characteristics of the irrigation waters blended in each experimental plot.

Irrigation waters	Year	EC_{iw} ($dS\,m^{-1}$)	$N—NH_4^+$ ($mmol_c\,L^{-1}$)	$N—NO_3^-$ ($mmol_c\,L^{-1}$)
Fresh waters	2007–2009	0.81	0.03	0.15
Saline waters	2007	7.60	0.03	0.15
	2008	9.60	0.03	0.15
	2009	10.60	0.03	0.15
Waters with nitrogen	2007	9.50	95.0	95.0
	2008	6.77	67.7	67.7
	2009	7.34	73.4	73.4

EC_{iw}, electrical conductivity of the irrigation water.

varying their discharge rates to obtain various mixtures between the three lines. Table 2 lists the different discharge rates of the emitters applying salts, nitrogen, and fresh water to each experimental plot. Table 3 presents the amount of saline waters, fresh waters, and waters with nitrogen applied in each experimental plot. The blended amounts thus varied between experimental plots, while the total amount of water applied per irrigation event and per crop season, as well as the quality of the irrigation waters before blending (Table 4), remained identical in all experimental plots.

The experimental field (Fig. 1) was thus divided into four groups (I–IV), each with three triple joint laterals, establishing a N gradient decreasing from group I to group IV. Each group was then divided into three sub-groups, A, B and C, each with a surface area of 6.75 m^2 (2.25 m wide × 3 m long), and with the Na^+ gradient decreasing from A to C. The emitters were spaced 1 m apart, with a total of nine dripping points in each of the 12 experimental plots. Two laterals of fresh water bordered the different groups (Fig. 1). Each sub-group area was bordered with earthen ridges, which prevented surface runoff from crossing over during rainfall and irrigation. The crop was irrigated three times per week from June to September with irrigation lasting 30–60 min per event. Fig. 2 presents daily irrigation rates that were applied during three irrigation seasons. Application amounts averaged 15, 16, and 17 mm per irrigation event in 2007, 2008, and 2009, respectively. Nitrogen fertilization was applied in four (2007), six (2008), and three (2009) irrigation events during the vegetative stage (July).

In the plots with the highest application of the synthetic saline waters (sub-group A), and those irrigated only with the locally available fresh water (sub-group C), TDR probes with waveguides from the Trase System (Soil Moisture Equipment Corp., Goleta, CA) and ceramic cups were installed at depths of 20, 40, and 60 cm to measure soil water contents and collect soil solutions, respectively. Only one TDR probe and one ceramic cup were installed in each depth. The soil solution was monitored for EC_{sw} and the concentrations of $N—NH_4^+$ and $N—NO_3^-$. Soil water content measurements and soil solutions were taken twice a week during irrigation seasons, generally 24 h after an irrigation event, and twice a month during the rest of the year.

The crop was harvested manually on September 27, 2007 (132 DAS), on September 30, 2008 (138 DAS), and on September 29, 2009 (137 DAS). The dry biomass of sweet sorghum was determined by harvesting all sorghum plants in each experimental plot and oven drying at 70 °C to a constant weight. Further details can be found in Ramos et al. (2012).

2.2. Modeling approach

Modeling of water flow and solute transport was carried out for all experimental plots included in sub-group A, irrigated with the highest application of synthetic saline waters, and in sub-group C, irrigated only with the water available in the region. The HYDRUS-2D software package (Šimůnek et al., 2006) was used to simulate the transient axisymmetrical (or radially symmetrical) three-dimensional movement of water and nutrients in the soil. In this approach, an individual emitter is represented as a point source located on the axis of rotation (Figs. 3 and 4). The axisymmetrical domain geometry representing the experimental conditions is shown in Fig. 4. The transport domain was set as a rectangle with a width of 37.5 cm (half the lateral spacing, i.e., the half-distance between triple joint laterals placed along the sorghum rows) and a depth of 100 cm. The transport domain was discretized into 2774 nodes, which corresponded to 5342 triangular elements (Fig. 4b). Observation nodes, corresponding to the locations where TDR probes and ceramic cups were installed, were placed at depths of 20, 40, and 60 cm, and at a radial distance of 20 cm away from the emitter source (Fig. 4a) and along the crop row (Fig. 3). A time-variable flux boundary condition was applied at the left part of the soil surface, approximately the first 20 cm to the right of the point emitter source, located at the top left corner of the soil domain (Fig. 4b). The flux boundary condition with the flux q was defined as:

$$q = \frac{\text{volume of water applied}}{\text{surface wetted area} \times \text{duration}} \quad (1)$$

where the volume of water applied (L^3) varied for different irrigation events, the surface wetted area (L^2) was approximately 1256 cm^2 (i.e., 3.14×20^2), and the irrigation duration was adjusted to permit water to infiltrate into the soil without producing positive surface pressure heads. The application time was divided into multiple intervals to allow for the application of irrigation waters of different qualities within a particular irrigation event. While the dripper discharge was constant and the irrigation duration variable in the experiment, for numerical convenience (and to avoid positive surface pressures, which sometimes existed in reality), we adjusted irrigation flux to produce the applied irrigation volume for a particular irrigation event, i.e., discharge rates of the emitters given in Table 2 were adjusted to apply the same volume of water but during longer time periods. Possible positive pressure heads at the flux boundary, which would make the numerical code unstable, were avoided by distributing the surface flux over a relatively large surface area and by spreading irrigation over a sufficient time period to allow water to infiltrate (from 0.2 to the entire day, depending on the volume applied). The atmospheric boundary condition was assumed for the remainder of the soil surface during periods with irrigation and for the entire soil surface during periods without irrigation. A no flow boundary condition was set at the left and right sections of the soil profile, so that no water and solute movement from neighboring emitters could be considered. A free drainage boundary condition was assumed at the bottom of the soil profile.

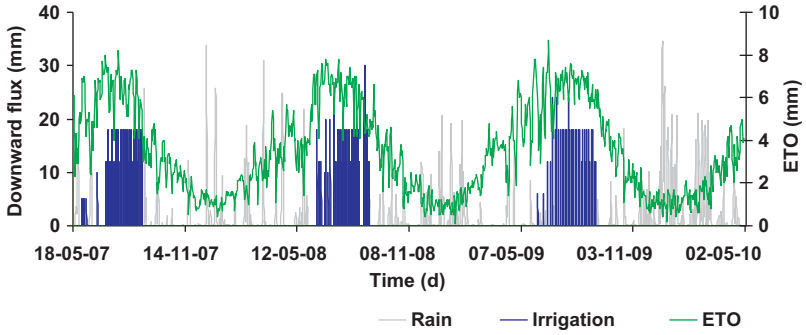

Fig. 2. Daily values of precipitation, irrigation, and reference evapotranspiration rates in Alvalade between 18th May 2007 and 2nd May 2010.

2.2.1. Water flow

The spatial distributions of transient soil water contents and volumetric fluxes were obtained using a numerical solution of the Richards equation for radially symmetric Darcian flow:

$$\frac{\partial\theta(h)}{\partial t} = \frac{1}{r}\frac{\partial}{\partial r}\left(r\,K(h)\frac{\partial}{\partial r}\right) + \frac{\partial}{\partial z}\left(K(h)\frac{\partial h}{\partial z} + K(h)\right) - S(r,z,t) \quad (2)$$

where θ is the volumetric soil water content ($L^3\,L^{-3}$), h is the soil water pressure head (L), t is time (T), r is the radial space coordinate (L), z is the vertical space coordinate (L), K is the hydraulic conductivity ($L\,T^{-1}$), and S is the sink term accounting for water uptake by plant roots ($L^3\,L^{-3}\,T^{-1}$). The unsaturated soil hydraulic properties were described using the van Genuchten–Mualem functional relationships (van Genuchten, 1980) as follows:

$$S_e(h) = \frac{\theta(h)-\theta_r}{\theta_s-\theta_r} = \frac{1}{(1+|\alpha\,h|^{\eta})^m} \quad (3)$$

$$K(h) = K_s S_e^{\ell}[1-(1-S_e^{1/m})^m]^2 \quad (4)$$

in which S_e is the effective saturation, θ_r and θ_s denote the residual and saturated water contents ($L^3\,L^{-3}$), respectively, K_s is the saturated hydraulic conductivity ($L\,T^{-1}$), α (L^{-1}) and η (–) are empirical shape parameters, $m = 1-1/\eta$, and ℓ is a pore connectivity/tortuosity parameter (–). The van Genuchten–Mualem parameters are presented in Table 1. They were obtained by fitting Eqs. (2) and (3) to laboratory data measured on undisturbed soil samples taken from a representative soil profile, as described in Ramos et al. (2011). The initial water content in the soil was set to a uniform value throughout the soil profile (Table 1). Since HYDRUS-2D simulations were started 2 weeks before the first irrigation event, the effects of the initial condition on long term simulations (2007–2010) of solute transport could be neglected.

2.2.2. Solute transport

Solute transport in a homogeneous porous medium and in a three-dimensional axisymmetrical domain was computed using the convection-dispersion equations (CDE) for each chemical species (EC_{sw}, $N{-}NH_4^+$, and $N{-}NO_3^-$) considered in our study, as follows:

$$\frac{\partial\theta\,c_k}{\partial t} + \rho\frac{\partial\bar{c}_k}{\partial t} = \frac{\partial}{\partial r}\left(\theta D_{rr}\frac{\partial c_k}{\partial r} + \theta D_{rz}\frac{\partial c_k}{\partial z}\right) + \frac{1}{r}\left(\theta D_{rr}\frac{\partial c_k}{\partial r} + \theta D_{rz}\frac{\partial c_k}{\partial z}\right) + \frac{\partial}{\partial z}\left(\theta D_{zz}\frac{\partial c_k}{\partial z} + \theta D_{rz}\frac{\partial c_k}{\partial z}\right) - \left(\frac{\partial q_r\,c_k}{\partial r} + \frac{q_r\,c_k}{r} + \frac{\partial q_z\,c_k}{\partial z}\right) + \phi_k - S\,c_{root,k} \quad (5)$$

where θ is the volumetric water content ($L^3\,L^{-3}$), c, $\bar{c}$, and c_{root} are solute concentrations in the liquid phase ($M\,L^{-3}$), solid phase ($M\,M^{-1}$), and sink term ($M\,L^{-3}$), respectively, ρ is the soil bulk density ($M\,L^{-3}$), q_r and q_z are the components of the volumetric flux density ($L\,T^{-1}$), D_{rr}, D_{zz}, and D_{rz} are the components of the dispersion tensor ($L^2\,T^{-1}$), ϕ represents chemical reactions of solutes involved in a sequential first-order decay chain ($M\,L^{-3}\,T^{-1}$), S is again the sink term accounting for water uptake by plant roots

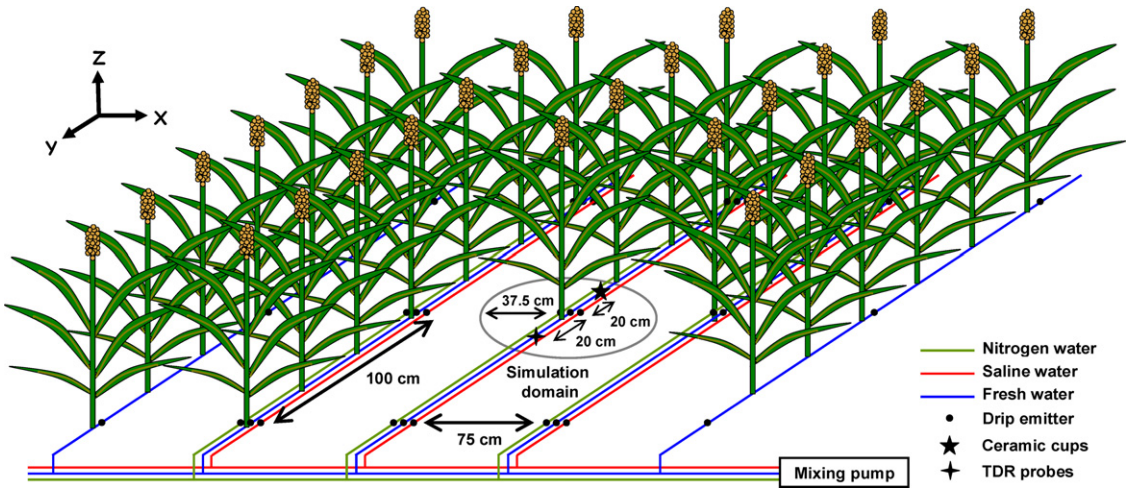

Fig. 3. Location of a point source emitter and monitoring sites in the experimental plot.

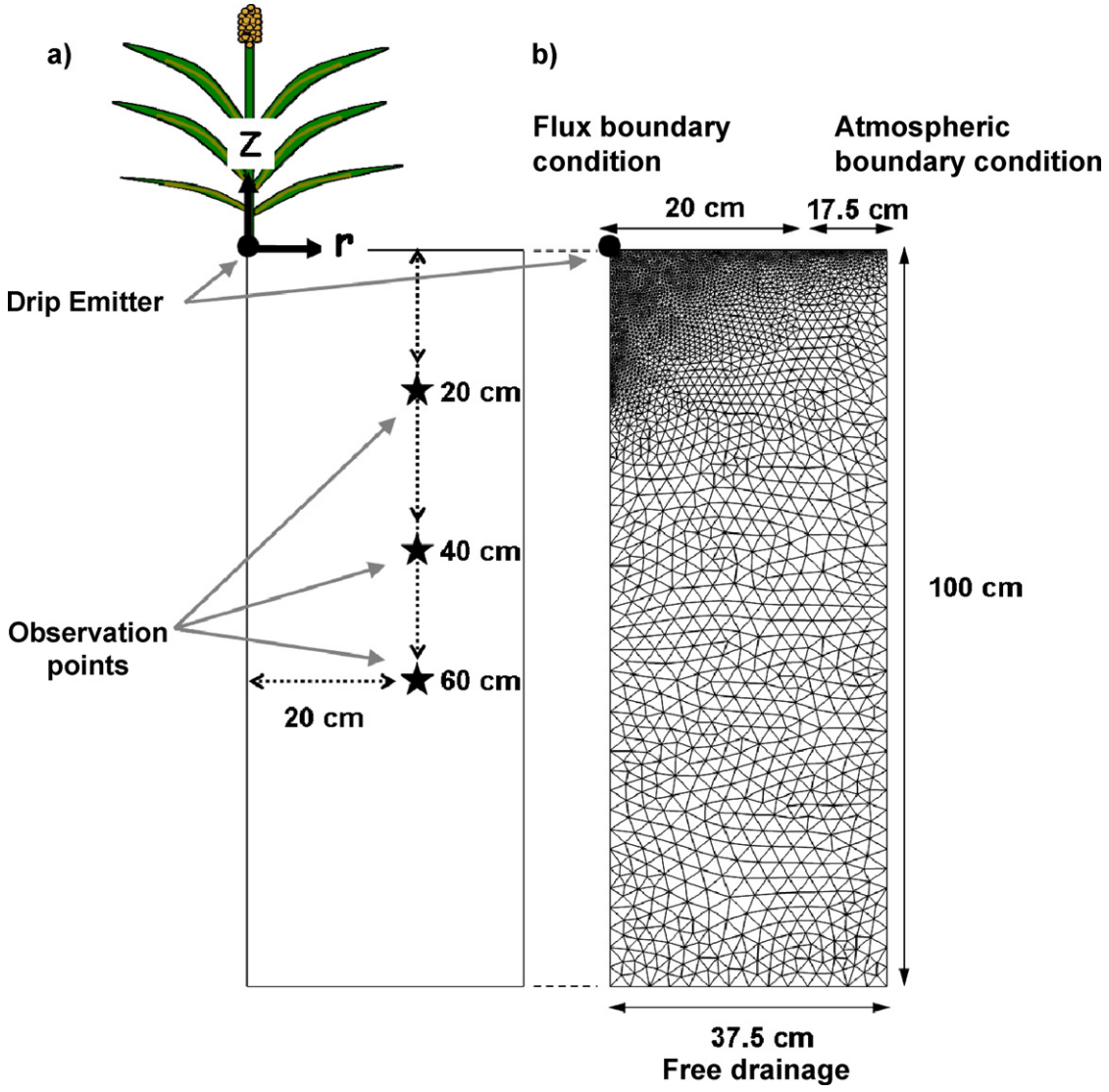

Fig. 4. Location of observation points within the soil profile (a) and an axisymmetrical domain geometry with the finite element discretization used in HYDRUS-2D simulations (b).

($L^3\,L^{-3}\,T^{-1}$), and subscript k represents chemical species present in our study (EC_{sw}, $N{-}NH_4^+$, and $N{-}NO_3^-$).

The components of the dispersion tensor are given by (Bear, 1972):

$$\begin{aligned}\theta D_{rr} &= \varepsilon_L \frac{q_r^2}{|q|} + \varepsilon_T \frac{q_z^2}{|q|} + \theta\tau D_0\\ \theta D_{zz} &= \varepsilon_L \frac{q_z^2}{|q|} + \varepsilon_T \frac{q_r^2}{|q|} + \theta\tau D_0\\ \theta D_{rz} &= (\varepsilon_L - \varepsilon_T)\frac{q_r q_z}{|q|}\end{aligned} \tag{6}$$

where $|q|$ is the absolute value of the volumetric flux density ($L\,T^{-1}$), ε_L and ε_T are the longitudinal and transversal dispersivities (L), D_0 is the molecular diffusion coefficient of the solute in free water ($L^2\,T^{-1}$), and τ is the tortuosity factor. Table 1 gives the ε_L values used in our study. They were obtained by fitting analytical solutions of the CDE to observed breakthrough data measured on undisturbed soil samples taken from a representative soil profile of Alvalade as described in Gonçalves et al. (2001). The value of ε_T was simply set as one tenth of ε_L (e.g., Mallants et al., 2011).

The distribution of solutes between the soil liquid and solid phases was related in Eq. (5) with the following linear adsorption isotherm:

$$\overline{c_k} = K_{d,k}\, c_k \tag{7}$$

where $K_{d,k}$ ($L^3\,M^{-1}$) is the distribution coefficient for the considered chemical species. Nitrate ($N{-}NO_3^-$) and EC_{sw} were assumed to be present only in the dissolved phase ($K_d = 0\,cm^3\,g^{-1}$), which simplified Eq. (5) for these two chemical species. Ammonium ($N{-}NH_4^+$) was assumed to adsorb to the solid phase according to Eq. (7) with the distribution coefficient K_d of 3.5 $cm^3\,g^{-1}$ (Hanson et al., 2006).

Since the fertilizer used in our study was NH_4NO_3, nitrification of the $N{-}NH_4^+$ species to $N{-}NO_3^-$ was assumed to be the main N process occurring in the soil. HYDRUS-2D incorporates this process in Eq. (5) by means of a sequential first-order decay chain as follows:

$$\phi_{N-NH_4^+} = -\phi_{N-NO_3^-} = -\mu_{w,N-NH_4^+}\theta\, c_{N-NH_4^+} - \mu_{s,N-NH_4^+}\rho\,\bar{c}_{N-NH_4^+} \tag{8}$$

where μ_w and μ_s are the first-order rate constants for solutes in the liquid and solid phases (T^{-1}), respectively. The first-order reaction

terms, representing nitrification of $N{-}NH_4^+$ to $N{-}NO_3^-$, thus act as a sink for $N{-}NH_4^+$ and as a source for $N{-}NO_3^-$. The values for μ_w and μ_s were set to be 0.2 d^{-1}. The parameters K_d, μ_w, and μ_s were taken from a review of published data presented by Hanson et al. (2006), and represent the center of the range of reported values.

The last term of Eq. (5) represents a passive root nutrient uptake, i.e., the movement of nutrients into roots by convective mass flow of water, directly coupled with root water uptake (Šimůnek and Hopmans, 2009). This term was defined as:

$$c_{root}(r, z, t) = \min[c(r, z, t), c_{max}] \quad (9)$$

where c_{max} is the *a priori* defined maximum concentration of the root solute uptake. Since we considered unlimited passive nutrient uptake for nitrogen species, c_{max} was set to a concentration value larger than the dissolved simulated concentrations, c, allowing all dissolved nutrients to be taken up by plant roots with root water uptake. Since for EC_{sw} a zero uptake was considered, c_{max} was set to zero.

2.2.3. Potential and actual evapotranspiration rates

The sink term (S) in Eqs. (2) and (5) was calculated using the macroscopic approach introduced by Feddes et al. (1978). In this approach, the actual local uncompensated root water uptake was obtained as follows (Feddes et al., 1978; van Genuchten, 1987; Skaggs et al., 2006a; Šimůnek and Hopmans, 2009):

$$S(h, h_\phi, r, z, t) = \alpha(h, h_\phi, r, z, t)S_p(r, z, t)$$
$$= \alpha(h, h_\phi, r, z, t)\beta(r, z, t)T_p(t)A_t \quad (10)$$

where $S_p(r,z,t)$ and $S(h,h_\phi,r,z,t)$ are the potential and actual volumes of water removed from a unit volume of soil per a unit of time ($L^3\,L^{-3}\,T^{-1}$), respectively, $\alpha(h,h_\phi,r,z,t)$ is a prescribed dimensionless stress response function of the soil water (h) and osmotic (h_ϕ) pressure heads ($0 \le \alpha \le 1$), $\beta(r,z,t)$ (L^{-3}) is a normalized root density distribution function, T_p is the potential transpiration rate (LT^{-1}), and A_t is the area of the soil surface associated with transpiration [L^2]. The actual transpiration rate, T_a (LT^{-1}), was then obtained by integrating Eq. (10) over the root domain, Ω (L^3), as follows:

$$T_a(t) = T_p(t)\int \Omega_r \alpha(h, h_\phi, r, z, t)\beta(r, z, t)d\Omega \quad (11)$$

The root distribution is defined in HYDRUS-2D according to Vrugt et al. (2001):

$$\Omega(r, z) = \left(1 - \frac{r}{r_m}\right)\left(1 - \frac{z}{z_m}\right)e^{-((p_r/r_m)|r^*-r|+(p_z/z_m)|z^*-z|)} \quad (12)$$

where r_m and z_m are the maximum radius and depth of the root zone (L), respectively, z^* and r^* are the locations of the maximum root water uptake in vertical and horizontal directions (L), respectively, and the p_r and p_z values are taken to be equal to one except for $r > r^*$ and $z > z^*$ when they become zero. The following parameters of the Vrugt et al. (2001) model were used in the simulations: r_m = 37.5 cm, z_m = 65 cm, r^* = 10 cm, z^* = 10 cm. We considered a simple root distribution model in which the roots of sweet sorghum expanded horizontally into all available space between sorghum lines (r_m = 37.5 cm), were concentrated mainly around the drip emitter (r^* = 10 cm, z^* = 10 cm) where water and nutrients were applied, and extended to a depth of 65 cm (z_m = 65 cm). We assumed that plants had no need of expanding their roots below this depth since water and nutrients were being applied at the soil surface and their life cycle lasted only five months. The parameters for defining the maximum root water uptake in vertical and horizontal directions (z and r^*) were also based on the scenarios developed by Gärdenäs et al. (2005) and Hanson et al. (2006, 2008). The selection of the maximum rooting depth was also based on the work carried out by Ramos et al. (2011) and the fact that root depths are relatively shallow under surface drip irrigation starting few days after sowing (Klepper, 1991; Allen et al., 1998; Zegada-Lizarazu et al., 2012). In addition, field observations carried out in November 2010 found no significant amounts of roots below this depth.

In this study we considered that during the growing seasons T_p rates were obtained by combining the daily values of reference evapotranspiration (ET_0), determined with the FAO Penman–Monteith method and the dual crop coefficient approach (Allen et al., 1998, 2005), as follows:

$$ET_c = (K_{cb} + K_e)ET_0 \quad (13)$$

where ET_c is the evapotranspiration (LT^{-1}), K_{cb} is the basal crop coefficient, which represents the plant transpiration component (–), and K_e is the soil evaporation coefficient (–).

Standard sweet sorghum K_{cb} values (Allen et al., 1998) were adjusted for the Alvalade climate, taking into consideration the crop height, wind speed, and minimum relative humidity averages for the period under consideration. The K_{cb} coefficient was further adjusted to account for the salinity and nitrogen stress, affecting sweet sorghum growth in each experimental plot, using the procedure for non-pristine agricultural vegetation (Allen et al., 1998):

$$K_{cb\,mid} = K_{c\,min} + (K_{cb\,full} - K_{c\,min})(1 - e^{(-0.7\,LAI)}) \quad (14)$$

where $K_{cb\ mid}$ is the estimated basal K_{cb} during mid-season when the leaf area index (LAI) ($L^2\,L^{-2}$) is smaller than for full cover conditions, $K_{cb\ full}$ is the estimated basal K_{cb} during mid-season (at the peak plant size or height) for vegetation having LAI > 3, and $K_{c\ min}$ is the minimum K_c for bare soil (0.15–0.20). For these estimations, LAI was monitored in each experimental plot during different stages of the sorghum cycle, using a non-destructive method to avoid removing plants from the experimental area. Length (L) and width (W) of crop leafs were measured on random plants grown in each experimental plot. These dimensions were then related to previously calibrated LAI values with the following equation:

$$LAI = 0.7586\sum_{i=1}^{n}(L \times W) \quad (15)$$

where LAI are the values measured using a LI-COR area meter (Model LI-3100C, LI-COR Environmental and Biotechnology Research Systems, Lincoln, NE) and n is the number of green leafs on each measured sorghum plant. Cubic splines were then fitted to LAI data to obtain a continuous function throughout the crop seasons.

The evaporation coefficient K_e was calculated as (Allen et al., 1998, 2005):

$$K_e = K_r(K_{c\,max} - K_{cb}) \le f_{ew}K_{c\,max} \quad (16)$$

where K_r is a dimensionless evaporation reduction coefficient dependent on the cumulative depth of water depleted (evaporated) from the topsoil, $K_{c\ max}$ is the maximum value of K_c (i.e., $K_{cb} + K_e$) after rain or irrigation, and f_{ew} is the fraction of the soil surface from which most evaporation occurs. Table 5 presents the crop coefficients and other crop related parameters estimated in each growing season.

During non-growing seasons, the procedure to estimate ET_c was greatly simplified by using the single crop coefficient approach and a K_c of 0.15 to account for a bare soil with a small percentage of weeds. Transpiration and evaporation were also separated as a function of leaf area index (Ritchie, 1972) using a fictitious LAI value of 1.0.

In all experimental plots, it was assumed that the potential root water uptake was reduced due to water stress as a result of the adopted irrigation schedule, which could lead to insufficient or

Table 5
Crop and soil parameters used for estimating plant transpiration and soil evaporation in each sorghum growing season.

Parameter	2007	2008	2009
Planting date	May 18	May 15	May 15
Harvest date	September 27	September 27	September 27
Av. wind speed ($m\,s^{-1}$)	2.2	2.4	2.3
Av. RH min (%)	26	32	24
Length stages (d):			
L_{ini}	63	64	64
L_{dev}	25	26	26
L_{mid}	24	25	25
L_{late}	21	24	23
f_w (irrigation)	0.3	0.3	0.3
REW (mm)	9	9	9
TEW (mm)	35.2	35.2	35.2
Z_e (cm)	15	15	15
LAI_{max} ($m^2\,m^{-2}$):			
Highest value	5.1	4.7	5.4
Plot	I-C	III-A	II-B
Lowest value	3.3	2.8	2.6
Plot	IV-B	IV-A	IV-A
$K_{cb\ ini}$	0.15	0.15	0.15
$K_{cb\ mid}$	1.23	1.21	1.24
$K_{cb\ end}$	1.07	1.06	1.09
$K_{cb\ full}$	0.15–1.23	0.15–1.21	0.15–1.24
$K_{c\ max}$	1.16–1.35	1.14–1.38	1.01–1.29

RH, relative humidity; L_{ini}, L_{dev}, L_{mid}, and L_{late}, length of crop initial, development, mid-season, and end season stages, respectively; f_w, fraction of soil surface wetted by irrigation (0.3–0.4: an interval used in calibration; an optimal value is given in the table); REW, readily evaporable water; TEW, total evaporable water, Z_e, depth of the surface soil layer that is subject to drying by way of evaporation (10–15 cm); LAI_{max}, maximum leaf area index measured in the experimental plots; $K_{cb\ ini}$, $K_{cb\ mid}$, and $K_{cb\ end}$, basal crop coefficient during crop initial, mid-season, and end season stages, respectively; $K_{c\ full}$, estimated basal K_{cb} during mid-season (at peak plant size or height) for vegetation having LAI > 3; $K_{c\ max}$, maximum value of K_c following rain or irrigation.

excessive supply of water to the crop. It was also assumed that the potential root water uptake was further reduced by osmotic stress, resulting from the use of blended saline water. The effects of water and salinity stresses were considered to be multiplicative as described by van Genuchten (1987) (i.e., $\alpha(h,h_\phi)=\alpha_1(h)\alpha_2(h_\phi)$ in Eq. (10)), so that different stress response functions could be used for the water and salinity stresses. Root water uptake reductions due to water stress, $\alpha_1(h)$, were described using the piecewise linear model proposed by Feddes et al. (1978). The water uptake is at the potential rate when the pressure head is between h_2 and h_3, drops off linearly when $h > h_2$ or $h < h_3$, and becomes zero when $h < h_4$ or $h > h_1$. The following parameters of the Feddes et al. (1978) model were used: $h_1 = -15$, $h_2 = -30$, $h_3 = -325$ to -600, $h_4 = -8000$ cm.

Root water uptake reductions due to salinity stress, $\alpha_2(h_\phi)$, were described by adopting the Maas (1990) salinity threshold and slope function. The salinity threshold (EC_T) for sweet sorghum corresponds to a value for the electrical conductivity of the saturation extract (EC_e) of 6.8 $dS\,m^{-1}$, and a slope (s) of 16% per $dS\,m^{-1}$. As required by HYDRUS-2D, these values were converted into EC_{sw} assuming that the EC_{sw}/EC_e ratio (k_{EC}) was 2, which is a common approximation used for soil water contents near field capacity in medium-textured soils (U.S. Salinity Laboratory Staff, 1954; Skaggs et al., 2006b).

2.3. Statistical analysis

Model validation was carried out by comparing field measured values with HYDRUS-2D simulations using various quantitative measures of the uncertainty, such as, the mean error (ME), mean absolute error (MAE) and the root mean square error (RMSE), given by:

$$\mathrm{ME} = \frac{1}{N}\sum_{i=1}^{N}(O_i - P_i) \tag{17}$$

$$\mathrm{MAE} = \frac{1}{N}\sum_{i=1}^{N}|O_i - P_i| \tag{18}$$

$$\mathrm{RMSE} = \sqrt{\frac{\sum_{i=1}^{N}(O_i - P_i)^2}{N-1}} \tag{19}$$

where O_i and P_i are observation values and model predictions in the units of a particular variable, and N is the number of observations.

The dual crop coefficient approach used here to estimate atmospheric demands requires various crop and soil parameters that need to be adjusted to particular experimental conditions. Therefore, these parameters, i.e., lengths of various growth stages, the basal crop coefficients during initial ($K_{cb\ ini}$), mid-season ($K_{cb\ mid}$) and end season ($K_{cb\ end}$) growth stages, the total evaporable water (TEW), the readily evaporable water (REW), the thickness of evaporation soil layer (Z_e), and the fraction of soil surface wetted by irrigation (f_w) were first calibrated by trial and error using HYDRUS-2D and the experimental data from the first crop season (2007), and then used to define the atmospheric demands for the second (2008) and third crop seasons (2009). The optimized parameters were considered to be calibrated when the RMSEs found for the soil water content, EC_{sw}, and N species were lower than those reported in Ramos et al. (2011), i.e., $RMSE_\theta < 0.04\ cm^3\,cm^{-3}$; $RMSE_{EC_{sw}} < 2.04\ dS\,m^{-1}$; $RMSE_{N-NH_4^+} < 0.07\ mmol_c\,L^{-1}$; and $RMSE_{N-NO_3^-} < 2.60\ mmol_c\,L^{-1}$. Ramos et al. (2011) used the one-dimensional version of HYDRUS (i.e., HYDRUS-1D, Šimůnek et al., 2008) and the single crop coefficient approach to simulate the same solutes for similar experimental conditions, albeit with a different crop. Therefore, when RMSEs obtained here with a more complex approach, i.e., using a dual crop coefficient procedure and a more appropriate geometrical description, were lower than those obtained previously with a simpler methodology, optimized parameters were considered to be calibrated. All other necessary HYDRUS-2D input material parameters,

such as soil hydraulic and solute transport parameters, were determined in the laboratory. Note that since our modeling approach is process-based, rather than conceptual, our input parameters can be obtained/measured independently. In general, we find that it is superior to measure input material parameters independently rather than fitting them. The correspondence between measurements and model predictions would have obviously been better, had the input parameters been fitted using numerical modeling. However, the model that can be successfully run with independently measured input material parameters is more robust for practical applications than calibrated models. Moreover, with this approach we not only validate the used modeling approach but also applied laboratory methodologies and various involved experimental procedures.

3. Results and discussion

3.1. Soil water balance

The HYDRUS-2D simulations began on May 18, 2007 and were carried out for the first crop and subsequent rainfall seasons (i.e., for 362 days) in order to calibrate the crop and soil parameters that were needed for estimating atmospheric demands using the dual crop coefficient approach. Table 6 presents the statistical indicators used to evaluate the level of agreement between water contents measured using TDRs and those simulated using the calibrated HYDRUS-2D model for three depths of plots I-A and I-C. The subsequent simulations with calibrated HYDRUS-2D began again on May 18, 2007 and were carried out continuously for the following 1078 days.

Fig. 5 shows the water contents measured at depths of 20, 40, and 60 cm in plots I-A and I-C, and compares these values with HYDRUS-2D simulations. Water contents increased to full saturation near the emitter after an irrigation or rain event, and then decreased gradually during the following hours and days, until the next irrigation or rain event took place. Deeper depths showed smaller water content variations since root water uptake and soil evaporation were more pronounced at shallower depths. Similar results were also obtained for the remaining plots (not shown). A ME of $-0.007\,cm^3\,cm^{-3}$ and a RMSE of $0.030\,cm^3\,cm^{-3}$ were found between measured and simulated water contents during the entire simulation period. Deviations between measured and simulated water contents can be attributed to different causes, including errors related to field measurements and to model input and model structure errors. They will be discussed below in detail.

Table 7 presents the output components of the soil water balance (i.e., potential transpiration, actual transpiration, soil evaporation, and percolation) in all experimental plots located in sub-groups A and C. The input components, i.e., irrigation and rainfall amounts, were already given in Section 2 and in Table 3. Since HYDRUS-2D does not have a crop growth module, the potential root water uptake (PRWU), i.e., potential transpiration (T_p) obtained in each experimental plot, was given as input for defining the atmospheric boundary conditions. T_p varied between 360 (plot IV-A, 2008) and 457 mm (plots I-C and II-A, 2009). Plots located in group IV, where no nitrogen was applied, generally had lower T_p values. In groups I–III, T_p averaged 394, 397, and 450 mm in 2007, 2008, and 2009, respectively. In group IV, T_p was lower, averaging 382, 379, and 413 mm during the same time periods. Considering that nitrogen requirements of sweet sorghum are relatively low (Barbanti et al., 2006), the amount of nitrogen applied in plot III (N1 = 130–190 kg/ha y^{-1} of N) was apparently sufficient to maximize T_p. Plots located in groups I and II may thus have experienced some 'luxury' uptake, i.e., a continued uptake of nitrogen beyond what was required for immediate growth.

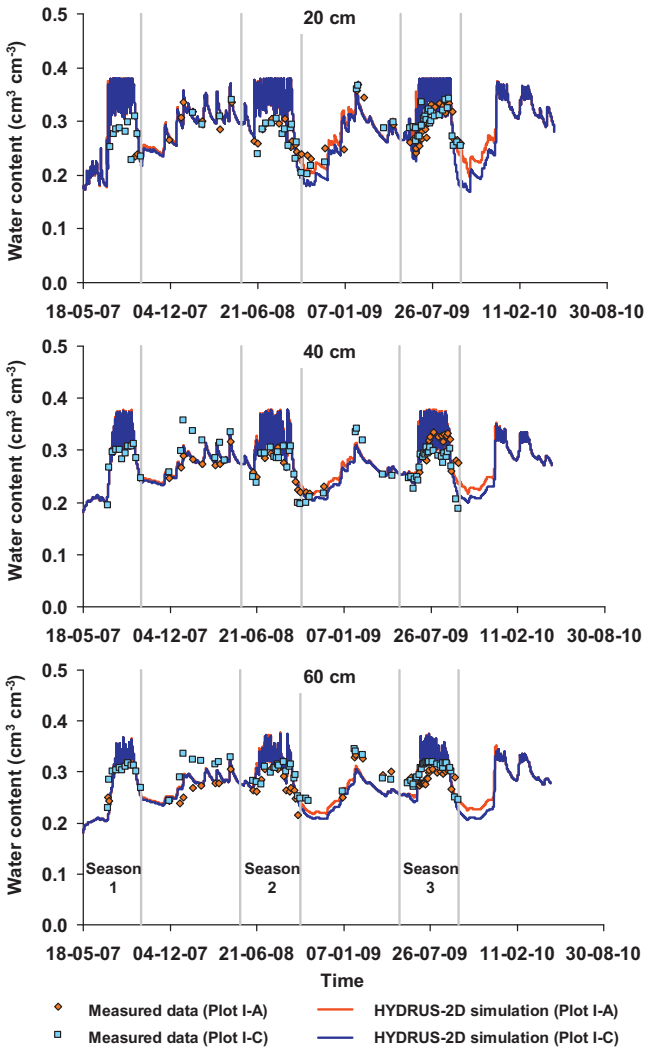

Fig. 5. Measured and simulated water contents at depths of 20 (top), 40 (middle), and 60 cm (bottom) in plots I-A and I-C.

T_p values obtained in plots irrigated with saline waters (sub-group A) were generally lower that those obtained in plots irrigated with fresh waters (sub-group C). However, the differences were found to be very small since sweet sorghum is moderately to highly tolerant to salinity, depending on the variety (Maas, 1990; Vasilakoglou et al., 2011). The largest T_p differences were found in 2009, in plots IV-A and IV-C (58 mm). Thus, in plot IV-A, the plant development was particularly affected by the continuous application of synthetic saline waters.

Apart from minor T_p variations found in the experimental plots, which resulted mainly from the differences in the spline functions fitted to the LAI measurements taken in each plot and in each crop season, T_p values estimated for sweet sorghum can be considered low. Ramos et al. (2011) estimated T_p for maize to vary between 600 and 800 mm. Water requirements estimated in this study for sweet sorghum are much lower than those for traditionally grown, irrigated crops in Portugal. Sweet sorghum thus seems to be a reasonable alternative crop to be grown in water scarce European Mediterranean regions.

Actual root water uptake, i.e., actual transpiration (T_a), as simulated by HYDRUS-2D, varied between 264 (plot IV-A, 2009) and 334 mm (plot I-C, 2009). T_p reductions due to water stress were a function of the adopted irrigation schedule. Within the same crop season, transpiration reductions were very similar since the

Table 6
Results of the statistical analysis between measured and simulated soil water contents, electrical conductivities of the soil solution (EC_{sw}), and $N—NH_4^+$, and $N—NO_3^-$ concentrations.

Statistic	Water content ($cm^3\ cm^{-3}$)	EC_{sw} ($dS\ m^{-1}$)	$N—NH_4^+$ ($mmol_c\ L^{-1}$)	$N—NO_3^-$ ($mmol_c\ L^{-1}$)
Data from 2007/2008 (calibration data):				
N	82	36	93	75
ME	−0.007	−0.216	0.029	−0.218
MAE	0.024	0.602	0.029	0.617
RMSE	0.033	0.854	0.042	1.253
Data from 2008/2010:				
N	276	211	241	263
ME	−0.007	−0.668	0.019	−1.668
MAE	0.023	1.255	0.026	2.244
RMSE	0.028	1.877	0.043	3.427
Data from 2007/2010 (all data):				
N	358	247	334	338
ME	−0.007	−0.602	0.022	−1.346
MAE	0.023	1.160	0.027	1.883
RMSE	0.030	1.764	0.042	3.078

N, number of observations; ME, mean error; MAE, mean absolute error; RMSE, root mean square error.

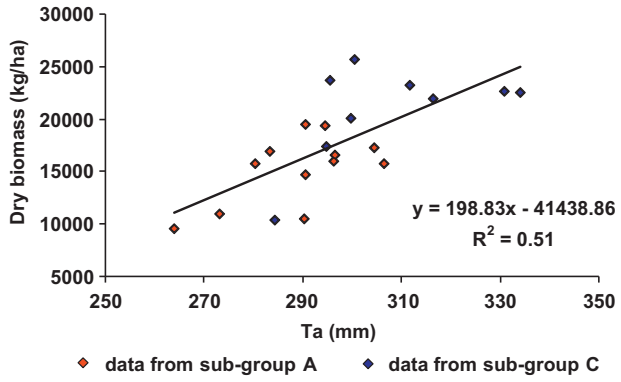

Fig. 6. Relationship between actual transpiration (T_a), as simulated by HYDRUS-2D, and dry biomass yield (Y).

irrigation schedule was the same in all experimental plots. In the plots located in sub-group C, irrigated only with fresh waters, T_p was reduced due to water stress by 25.3–27.4%, 21.9–22.8%, and 26.3–26.9% in 2007, 2008, and 2009, respectively. Water stress was thus a function of the adopted irrigation schedule during each season and did not vary among experimental plots.

In plots located in sub-group A (irrigated with saline waters), T_p was further reduced due to salinity stress. During 2007, T_a estimated for the different plots included in sub-group A was generically the same as in sub-group C (irrigated with fresh waters), i.e., sweet sorghum showed to be tolerant to the levels of salinity reached in the soil solution of all experimental plots irrigated with fresh or synthetic saline waters. However, in 2008 and 2009, T_p suffered reductions (in sub-group A) of 24.2–26.9%, and 31.3–33.3%, respectively, due to the combined effects of water and salinity stresses, i.e., 2.3–4.7% (in 2008) and 4.6–7.0% (in 2009) higher than T_p reductions found in the plots irrigated only with fresh waters (sub-group C). In the following years, the salinity stress thus became increasingly higher (in sub-group A). Hence, soil salinization and the increase of the salinity stress was related to the continuous and increasing amount of synthetic saline waters being applied in each experimental plot.

Fig. 6 relates actual transpiration T_a calculated using HYDRUS-2D with the experimentally determined sorghum yield (Y), given in terms of dry biomass, by means of the empirical relationship, $Y=f(T_a)$. This relationship, generally thought to be approximately linear, is valid for a particular plant (canopy) at a particular site subject to standard tillage and nutrition conditions (Novák and van Genuchten, 2008). The relation found in our study was somewhat poor, with the agreement between T_a and dry biomass reaching R^2 of only 0.51. Since HYDRUS-2D does not account for a crop growth module, this result was not particularly surprising. Nevertheless, had water been the only limiting factor in our experiment, the relation would likely have been better. However, this could not be easily observed in our study since the amount of water applied per year was the same, while the total water depths applied during each crop season were apparently not different enough to establish a closer relation. The relation in Fig. 6 essentially resulted from the effects that water quality had on T_a and crop yield. While plots irrigated with fresh water (sub-group C) had higher sorghum yields and T_a values, plots irrigated with saline waters (sub-group A) had lower sorghum yields and T_a values (Fig. 6). Nitrogen also did not influence the $Y(T_a)$ relation since N stress at a given period can mainly affect sorghum yield, while LAI, and consequently T_a, remain high.

Finally, the soil water balance (Table 7) in each experimental plot shows relatively high percolation. Percolation reached 162–174, 292–299, and 292–309 mm in 2007, 2008, and 2009, respectively. These values correspond to 31–34%, 50–51%, and 51–54% of the water applied during crop seasons, i.e., from sowing to harvest. While percolation was expected to be large, since application rates during irrigation seasons were high, the values estimated for crop seasons of 2008 and 2009 may be somewhat deceiving. They result from running HYDRUS-2D continuously for the entire simulation period. Since cumulative percolation obtained during the entire simulation period (2007–2010) only reached 36–37% of the applied water, and considering that root water uptake was much higher during crop seasons, percolation in 2008 and 2009 also accounted for the water stored below the root zone. Therefore, we ended up not being able to actually quantify percolation due to the adopted irrigation schedule, since the water balance evaluated for each crop season also accounted for the water that was no longer accessible to plants. Nevertheless, the effects of nitrogen applications and water quality on drainage were small. Plots with higher root water uptake showed generally lower percolation.

3.2. Salinity build-up and distribution

Fig. 7 shows EC_{sw} measured at the 20, 40, and 60 cm depth in plots I-A and I-C, and compares these values with HYDRUS-2D simulations. Similar results were also found for the remaining plots of sub-groups A and C. Within the same sub-group (Fig. 1), EC_{sw} varied due to the effect of nitrogen fertigation on root water uptake.

Table 7
Output components of the soil water balance in each experimental plot.

Sub-plot	Group I				Group II				Group III				Group IV			
	T_p (mm)	T_a (mm)	E (mm)	P (mm)	T_p (mm)	T_a (mm)	E (mm)	P (mm)	T_p (mm)	T_a (mm)	E (mm)	P (mm)	T_p (mm)	T_a (mm)	E (mm)	P (mm)
Season 1 (2007)																
A	386	280	173	162	391	294	170	167	394	296	168	168	384	290	174	168
C	399	298	163	170	396	297	164	172	395	295	169	173	380	284	177	174
Season 2 (2008)																
A	398	291	191	292	383	283	200	295	402	296	190	294	360	273	207	296
C	406	316	192	293	390	301	197	299	404	312	192	298	398	311	192	299
Season 3 (2009)																
A	456	307	172	292	457	305	170	294	434	291	183	299	384	264	206	302
C	457	334	174	298	449	331	177	302	449	328	176	309	442	324	181	309
Cumulative fluxes (2007–2010)																
A	1382	982	–	1101	1374	981	–	1107	1373	983	–	1111	1270	930	–	1119
C	1401	1065	–	1083	1377	1045	–	1097	1390	1051	–	1102	1363	1036	–	1105

T_p, potential transpiration; T_a, actual transpiration; E, evaporation; P, percolation.

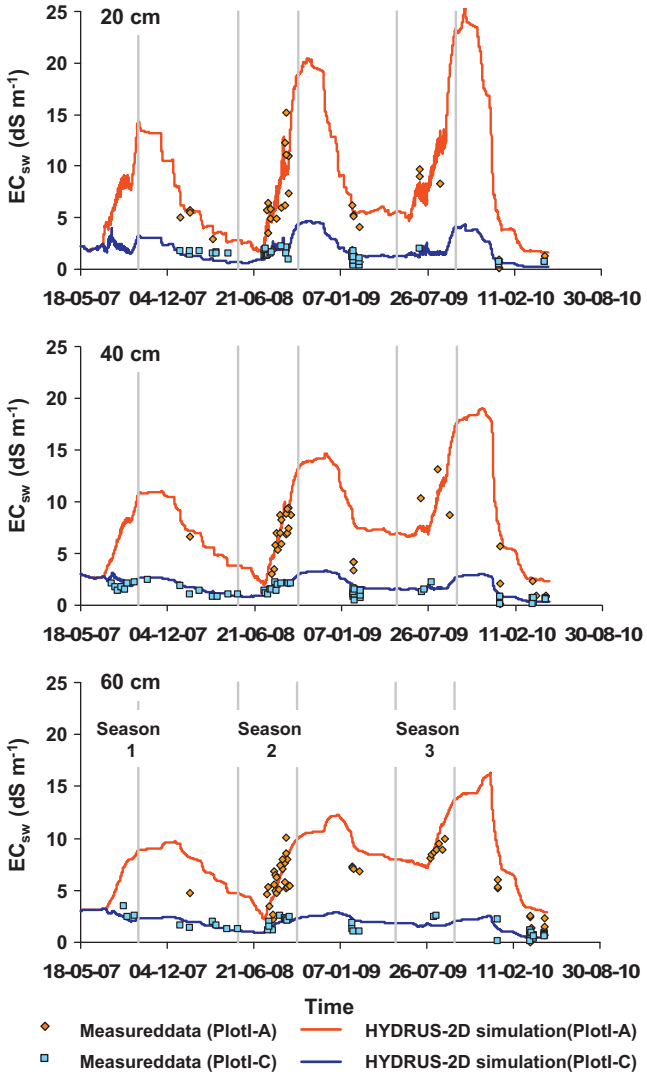

Fig. 7. Measured and simulated electrical conductivities of the soil solution at 20 (top), 40 (middle), and 60 cm (bottom) depth in plots I-A (irrigated with the highest application of synthetic saline waters) and I-C (irrigated with fresh waters only).

Between sub-groups (but within the same group), EC_{sw} varied due to the effect of water quality on root water uptake.

The statistical indicators (Table 6) obtained while comparing measured and simulated EC_{sw} for three depths of all plots in sub-groups A and C resulted in a ME of $-0.602\,dS\,m^{-1}$ and a RMSE of $1.764\,dS\,m^{-1}$.

Figs. 8 and 9 show the simulated distributions of EC_{sw} in plots I-A and I-C, respectively, at the beginning and at the end of each crop season. Based on model simulations, the continuous use of synthetic saline irrigation waters led to soil salinization in plot I-A over the years (Fig. 8). At harvest, simulations showed that EC_{sw} increased considerably to values above $24\,dS\,m^{-1}$ in the region around the drip emitter. At the beginning of each crop season that essentially correspond to the end of the rainfall leaching periods, simulated EC_{sw} values were also increasingly higher throughout the years, especially at deeper depths.

Considering that the Maas (1990) salinity threshold parameter for sweet sorghum corresponds to EC_{sw} of $13.2\,dS\,m^{-1}$ ($EC_e = 6.8\,dS\,m^{-1}$; $k_{EC} = 2$), the part of the soil domain with EC_{sw} above this threshold was already considerable during harvest in 2007. However, EC_{sw} only increased above the threshold EC_{sw} near the end of the crop season when irrigation ceased and the soil dried

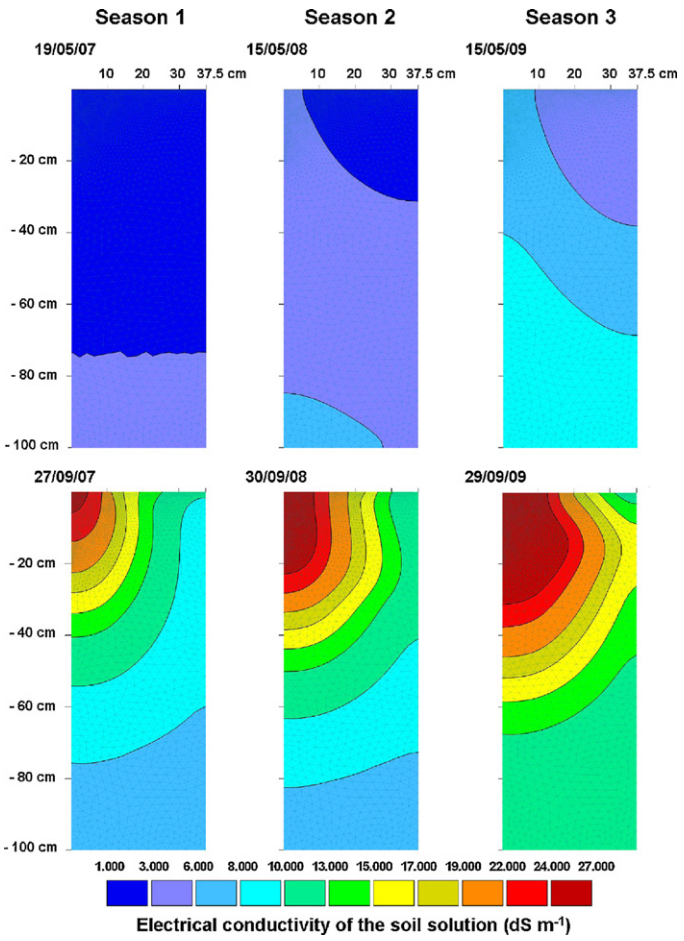

Fig. 8. Simulated distributions of the electrical conductivity of the soil solution in plot I-A (irrigated with synthetic saline waters) during sowing (top) and harvest (bottom) of each crop season. The drip emitter was located in the top left corner of each contour plot.

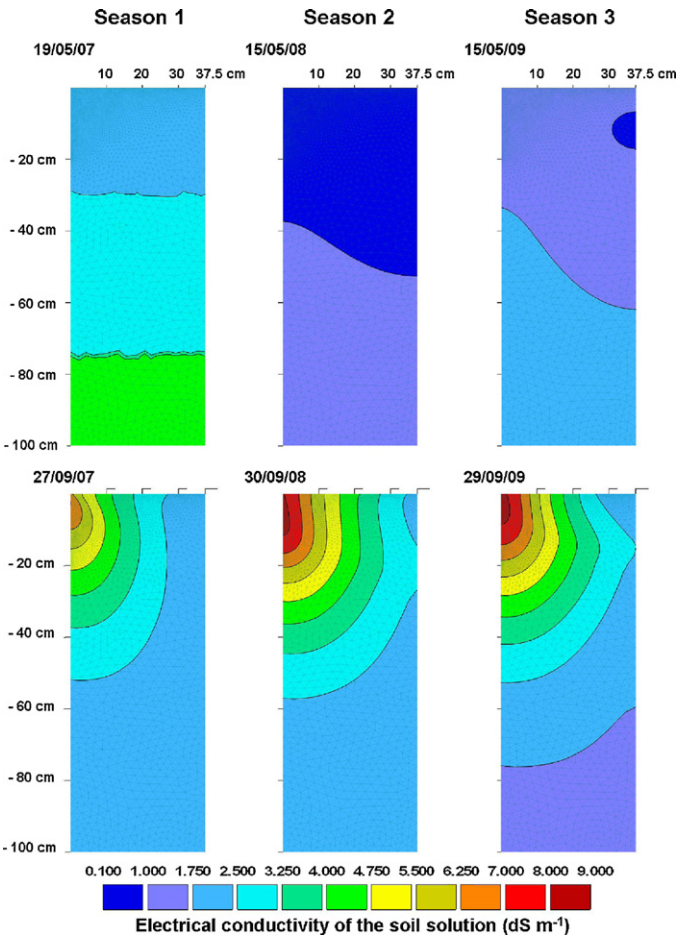

Fig. 9. Simulated distributions of the electrical conductivity of the soil solution in plot I-C (irrigated with fresh waters only) during sowing (top) and harvest (bottom) of each crop season. The drip emitter was located in the top left corner of each contour plot.

out (Fig. 7). Therefore, transpiration was not significantly reduced due to the salinity stress during that year (Table 7). In 2008 and 2009, the threshold value was reached earlier, with the region around the drip emitter with EC_{sw} values above 13.2 dS m^{-1} being much larger than in 2007. Hence, transpiration was increasingly reduced due to the salinity stress as a result of the accumulation of salts in the soil domain.

On the other hand, irrigation with fresh waters, having a relatively low salinity (EC_{iw} > 0.8; Table 4), also led to larger EC_{sw} at the end of each crop season, but the levels reached were always lower than 9 dS m^{-1} and decreased significantly due to rainfall leaching (Fig. 9). Therefore, in sub-group C, root water uptake was not affected by the salinity stress.

3.3. Nitrogen balance

Fig. 10 shows N—NH_4^+ and N—NO_3^- concentrations measured at a depth of 20, 40, and 60 cm in plots I-C and IV-C, and compares these values with HYDRUS-2D simulations. Figs. 11 and 12 show the simulated distributions of N—NH_4^+ and N—NO_3^- concentrations in plot I-A during the second crop season. In groups I through IV, N—NH_4^+ and N—NO_3^- concentrations varied according to the amounts of nitrogen applied in each experimental plot. In sub-group A-C (but within the same group), N—NH_4^+ and N—NO_3^- concentrations varied due to the effects of water quality on root water uptake.

The statistical indicators (Table 6) obtained while comparing measured and simulated N—NH_4^+ concentrations for three depths, and for all experimental plots located in sub-groups A and C, showed a ME of 0.022 mmol$_c$ L^{-1} and a RMSE of 0.042 mmol$_c$ L^{-1}. Corresponding statistical indicators for N—NO_3^- concentrations resulted in a ME of −1.346 mmol$_c$ L^{-1} and a RMSE of 3.078 mmol$_c$ L^{-1}.

Table 8 shows the nitrogen balances evaluated for each experimental plot during the three crop seasons included in the simulation period. While most components of the nitrogen balance were restricted to the duration of a crop season, leaching was calculated to also include the solute mass lost during the subsequent rainfall period. Nitrogen leaching was directly related to water flow through the bottom boundary of the soil domain. Therefore, since the percolation component of the water balance was high, so was the nitrogen leaching component here. The movement of N out of the root zone also depended on the amount of applied N, the form of N in the fertilizer, and the time and number of fertigation events.

Based on model simulations, most of the applied N—NH_4^+ was rapidly nitrified into N—NO_3^-, not reaching depths deeper than 20 cm and not being significantly taken up by plant roots. On the one hand, N—NH_4^+ adsorbs to the solid phase and thus its movement is significantly retarded compared to N—NO_3^-, and on the other hand, due to rapid nitrification, it does not stay long enough in the root zone to be taken up by plant roots. Fig. 11 exemplifies how, based on model simulations, N—NH_4^+ concentrations never increased at depths below 20 cm during the crop season of 2008. Also, at the

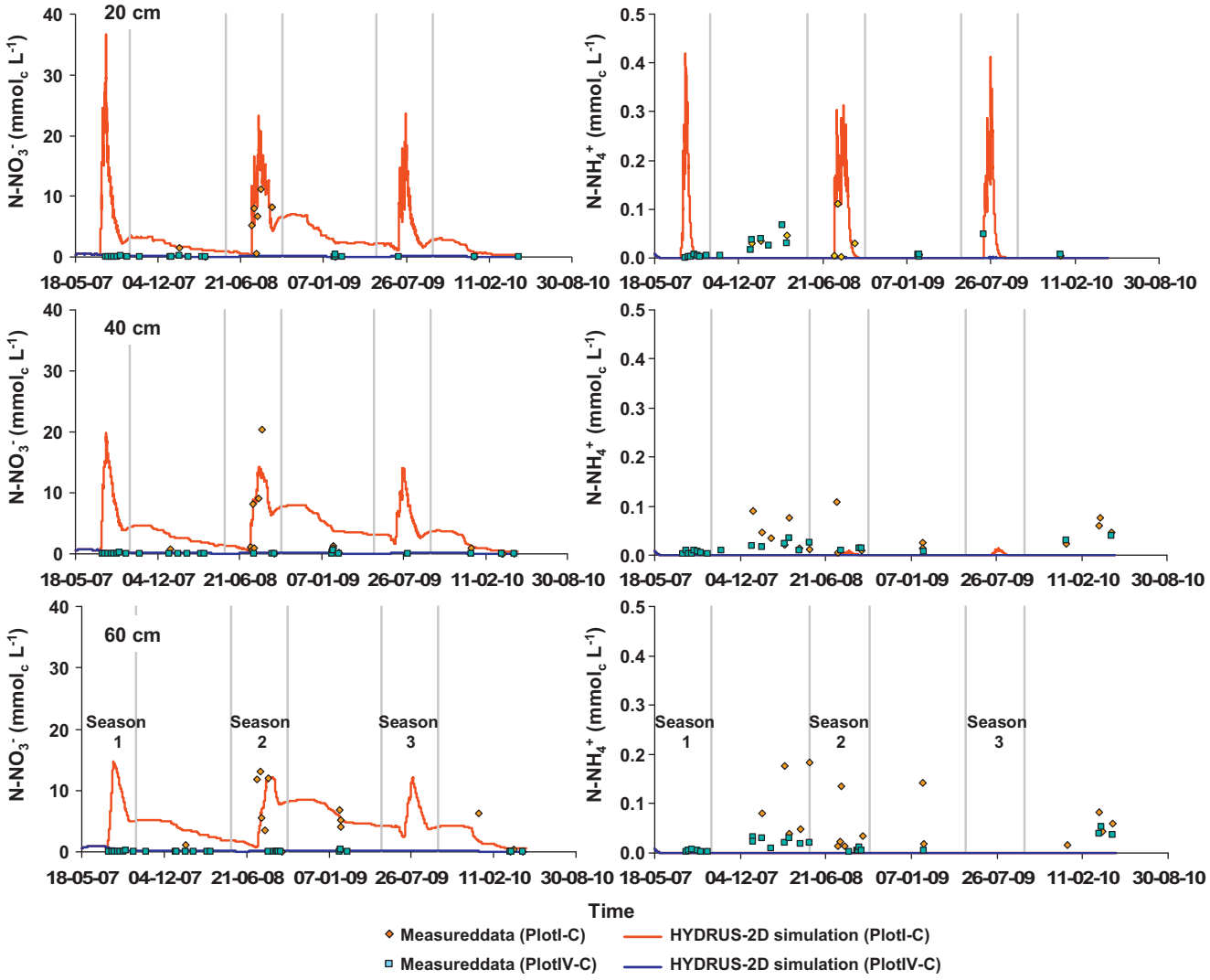

Fig. 10. Measured and simulated $N—NO_3^-$ (left) and $N—NH_4^+$ (right) concentrations at 20 (top), 40 (middle), and 60 cm (bottom) depth in plots I-C (the highest application of N) and I-C (no fertigation events).

end of the irrigation season (September 6, 2008), $N—NH_4^+$ concentrations in the soil profile were already very low. Leaching of nitrogen occurred mainly in the $N—NO_3^-$ form. Fig. 12 shows relatively high $N—NO_3^-$ concentrations below the root zone (>65 cm) during the entire crop season of 2008. $N—NO_3^-$ leaching reached 41–70% of the total amount of $N—NO_3^-$ available in the soil system, whether it came from direct application or from $N—NH_4^+$ nitrification. The higher the number of fertigation events, the lower the amount of N applied per event, and thus the lower the amount of leached $N—NO_3^-$. In 2007, when nitrogen was applied in only four fertigation events, $N—NO_3^-$ leaching varied between 51% and 53% of the total amount of $N—NO_3^-$ available in the soil system. In 2008, when nitrogen was applied in six fertigation events, only 41% of the total amount of available $N—NO_3^-$ leached. Finally, in 2009, when only three fertigation events took place, 68–70% of the total amount of available $N—NO_3^-$ was leached. Since $N—NH_4^+$ was rapidly nitrified and $N—NO_3^-$ easily leached, model simulations produced relatively low concentrations of both solutes in the soil profile at harvest and at the beginning of the following year's crop season. Simulations were thus in agreement with $N—NH_4^+$ and $N—NO_3^-$ concentrations measured in the saturation extract of samples collected at 20, 40, and 60 cm depth of every experimental plot. Experimental $N—NH_4^+$ concentrations were always lower than 0.17 $mmol_c\ L^{-1}$, while $N—NO_3^-$ concentrations reached a maximum value of 10.28 $mmol_c\ L^{-1}$ in deeper soil layers.

Nutrient uptake by plant roots occurred mainly in the $N—NO_3^-$ form as well. The number of fertigation events also significantly influenced the amount of $N—NO_3^-$ taken up by plant roots. Nutrient uptake varied between 23% and 42% of the total amount of $N—NO_3^-$ available in the soil system. In 2007, $N—NO_3^-$ uptake reached 37% of the applied $N—NO_3^-$. In 2008, with two additional fertigation events, nutrient uptake increased to 39–42% of the applied $N—NO_3^-$. Finally, in 2009, with only three fertigation events, $N—NO_3^-$ uptake decreased to values between 23% and 25% of the total amount of available $N—NO_3^-$. The higher number of fertigation events also led to higher yields. The average dry biomass yield measured in all plots with the N supply (groups I-III) was 19.3, 20.4, and 18.3 ton/ha in 2007, 2008, and 2009, respectively. However, in this last analysis we have to also take into consideration the increase in the salinity stress from one crop season to the next in plots irrigated with saline waters, which negatively influenced the crop yield.

The effects of the salinity stress on nutrient uptake (and inversely on nutrient leaching) was relatively small since sweet sorghum has a medium to high tolerance to salinity, and consequently there were only small reductions in transpiration due to the

Table 8
Nitrogen balance in each experimental plot during the three crop growth seasons.

Plot	$N—NH_4^+$ $soil_{Initial}$ (kg/ha)	$N—NH_4^+$ applied (kg/ha)	$N—NH_4^+$ leached (kg/ha)	$N—NH_4^+$ adsorbed (kg/ha)	$N—NH_4^+$ sorghum uptake (kg/ha)	$N—NH_4^+$ weeds uptake (kg/ha)	$N—NH_4^+$ decay (kg/ha)	$N—NH_4^+$ $soil_{end}$ (kg/ha)	$N—NO_3^-$ $soil_{Initial}$ (kg/ha)	$N—NO_3^-$ applied (kg/ha)	$N—NO_3^-$ leached (kg/ha)	$N—NO_3^-$ sorghum uptake (kg/ha)	$N—NO_3^-$ weeds uptake (kg/ha)	$N—NO_3^-$ $soil_{end}$ (kg/ha)	Mass balance error[a] (kg/ha)
Group I															
Season 1 (2007)															
A	5	259	0	1	3	0	259	0	10	266	271	198	6	104	4.03
C	5	259	0	1	3	0	259	0	10	266	272	200	6	101	3.77
Season 2 (2008)															
A	0	286	0	1	5	0	280	0	38	295	249	245	13	152	4.05
C	0	286	0	1	5	0	280	0	37	295	248	250	17	144	2.74
Season 3 (2009)															
A	0	208	0	1	2	0	205	0	81	217	350	118	3	76	4.20
C	0	208	0	0	2	0	206	0	81	217	350	123	6	69	2.84
Cumulative masses (2007–2010)															
A	5	753	0	4	10	0	744	0	10	777	870		583	11	4.36
C	5	753	0	2	10	0	746	0	10	777	870		600	11	3.37
Group II															
Season 1 (2007)															
A	5	174	0	1	2	0	175	0	10	180	185	135	4	71	4.10
C	5	174	0	1	2	0	175	0	10	181	186	135	4	69	3.73
Season 2 (2008)															
A	0	192	0	1	3	0	187	0	26	200	171	161	9	106	3.86
C	0	192	0	1	3	0	188	0	26	200	169	166	12	100	2.61
Season 3 (2009)															
A	0	139	0	1	1	0	136	0	56	148	231	80	2	51	6.01
C	0	139	0	1	1	0	137	0	56	148	231	82	4	47	4.71
Cumulative masses (2007–2010)															
A	5	504	0	3	7	0	499	0	10	528	586		392	7	4.99
C	5	504	0	2	7	0	500	0	10	529	586		403	7	3.99
Group III															
Season 1 (2007)															
A	5	87	0	0	1	0	90	0	10	94	100	73	2	38	2.44
C	5	87	0	0	1	0	90	0	10	94	102	72	2	38	1.84
Season 2 (2008)															
A	0	97	0	0	2	0	95	0	14	106	87	88	5	54	2.34
C	0	97	0	0	2	0	95	0	14	106	88	90	6	52	1.07
Season 3 (2009)															
A	0	71	0	0	1	0	70	0	29	80	125	42	1	29	3.59
C	0	71	0	0	1	0	70	0	29	80	124	45	2	26	2.18
Cumulative masses (2007–2010)															
A	5	254	0	1	3	0	255	0	10	279	312		211	4	2.87
C	5	254	0	1	3	0	255	0	10	279	314		217	4	1.62
Group IV															
Season 1 (2007)															
A	5	2	0	0	0	0	6	0	10	9	16	7	0	5	1.94
C	5	2	0	0	0	0	6	0	10	9	16	7	0	5	1.70
Season 2 (2008)															
A	0	2	0	0	0	0	2	0	2	11	8	4	0	4	3.19
C	0	2	0	0	0	0	2	0	2	11	7	5	0	3	2.00
Season 3 (2009)															
A	0	2	0	0	0	0	2	0	2	12	10	4	0	4	3.27
C	0	2	0	0	0	0	2	0	2	12	9	5	0	3	1.52
Cumulative masses (2007–2010)															
A	5	6	0	0	0	0	11	0	10	32	33		16	1	3.33
C	5	6	0	0	0	0	11	0	10	32	32		18	1	2.24

[a] Mass balance error $= \left(\frac{\sum N_{input} - \sum N_{output}}{\sum N_{input} \times 100} \right)$.

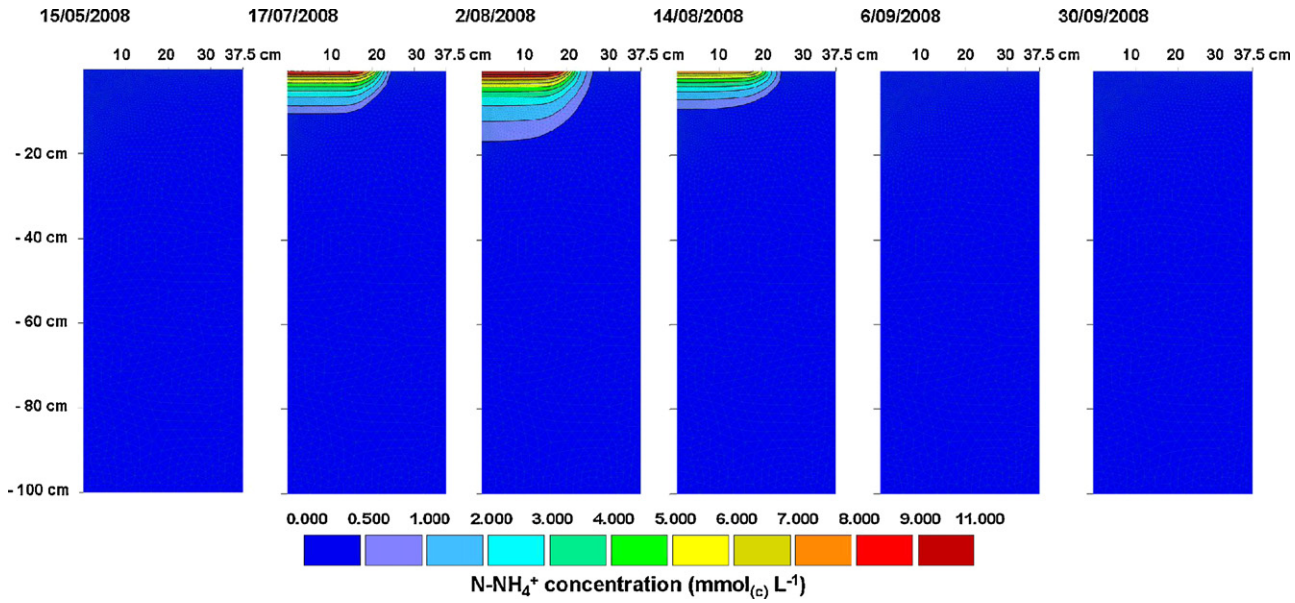

Fig. 11. Simulated distributions of N—NH_4^+ concentration in plot I-A during crop season 2, after sowing (May 15, 2008), after the first fertigation event (July 17, 2008), after the forth fertigation event (August 2, 2008), after the sixth and last fertigation event (August 14, 2008), at the end of the irrigation period (September 9, 2008), and at harvest (September 30, 2008). The drip emitter was located in the top left corner of each contour plot.

increase of the osmotic stress. Although nutrient uptake was somewhat lower in the plots irrigated with saline waters, only in group I, which had the highest applications of nitrogen, were the differences in N uptake between plots larger. However, even here, the difference in the cumulative N uptake between plots I-A and I-C was only 17.9 kg/ha. This was not significant enough to conclude that one could save on nitrogen applications by considering the quality of the irrigation water when defining an optimum fertigation schedule.

Fig. 13 shows the relationship between the N—NO_3^- plant uptake calculated using HYDRUS-2D and the experimentally determined dry biomass yield expressed using a logarithmic function with a R^2 of 0.71. This logarithmic function fitted to experimental data shows that an additional incremental increase of N—NO_3^- uptake produces diminishing returns in the total dry biomass response. Each additional unit of N—NO_3^- taken up by plant roots added less to the total biomass output than the previous unit did. After a certain level of N—NO_3^- uptake was reached (estimated here to be between those registered for groups II-III, i.e., 130–180 kg/ha), further increases in nutrient uptake did not contribute directly to the increase of the dry biomass yield. Group I thus involved some 'luxury' uptake, since the amount of N—NO_3^- taken up by plant roots did not contribute significantly to the dry biomass yield. More detailed results of the effect of brackish waters on nitrogen needs and dry biomass yield of sweet sorghum can be found in Ramos et al. (2012).

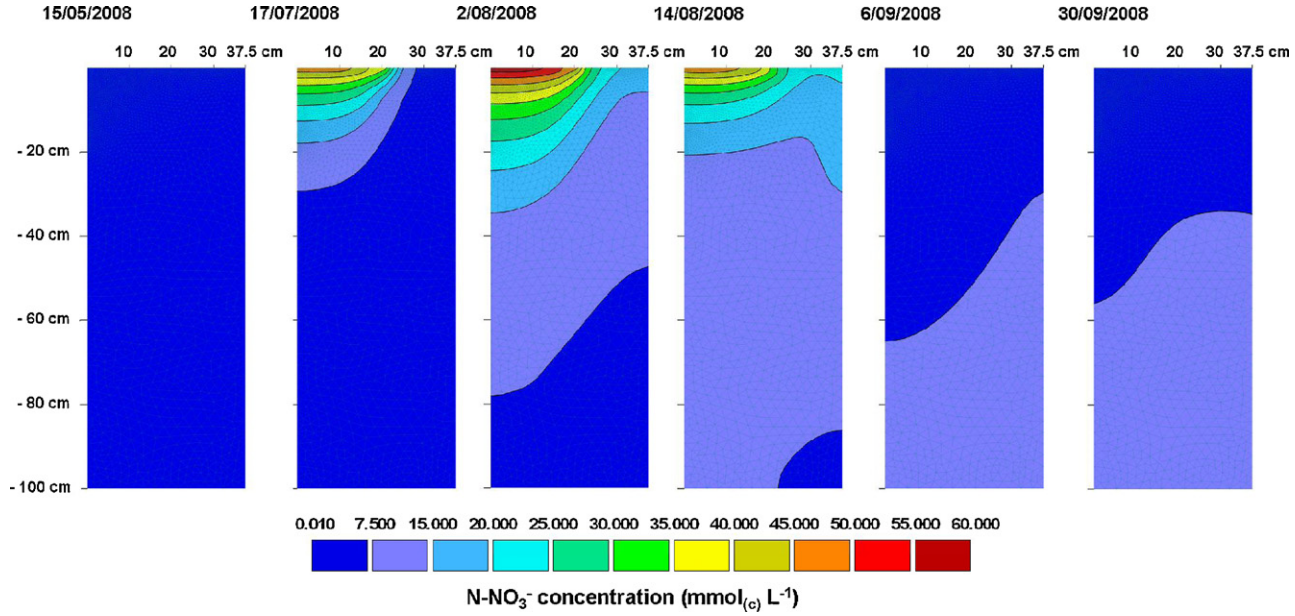

Fig. 12. Simulated distributions of N—NO_3^- concentration in plot I-A during crop season 2, after sowing (May 15, 2008), after the first fertigation event (July 17, 2008), after the forth fertigation event (August 2, 2008), after the sixth and last fertigation event (August 14, 2008), at the end of the irrigation period (September 9, 2008), and at harvest (September 30, 2008). The drip emitter was located in the top left corner of each contour plot.

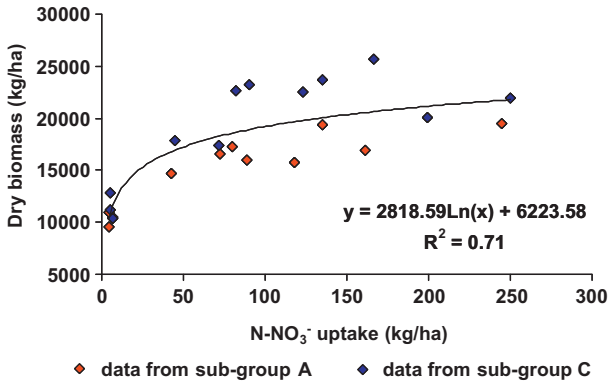

Fig. 13. Relationship between N—NO_3^- uptake, as simulated by HYDRUS-2D, and dry biomass yield (Y).

3.4. About model validation

Deviations between measured data and simulated variables (Table 6) can be attributed to different causes, including errors related to field measurements, and to model input and model structure errors.

Field measurements: The most relevant source of errors related to field measurements refers to the representativeness of TDR measurements and ceramic cup samplings at different depths. TDR probes measure spatially averaged water contents over a certain soil volume, the size of which depends on the size and orientation of TDR probes (Ferré et al., 2002). However, the distribution of water under drip irrigation is highly spatially non-uniform (Gärdenäs et al., 2005; Hanson et al., 2006). Water contents were highest near the drip emitter after an irrigation event and then redistributed throughout the soil profile. Therefore, TDR probes averaged water contents over soil regions with different moisture status, while HYDRUS-2D reports water contents for a precise soil location (Fig. 4). Note that due to the dimensionality (axisymmetrical) of our calculations, by averaging water content over a certain area around the observation node, we would obtain an average value for a circular pipe, rather than for a straight cylinder over which TDR averages its measurements. Likewise, measurements taken with suction cups were averaged over a sampling area of a certain volume, the size of which depends on soil hydraulic properties, the soil water content, and the applied suction in the ceramic cup (Weihermüller et al., 2005, 2011). Measured values thus did not represent point values as the simulations did. Spatial soil variability can also affect concentrations measured by suction cups, an issue extensively studied by Weihermüller et al. (2011).

Model input errors: The accuracy of the soil hydraulic properties, which were measured on undisturbed soil samples taken not in each experimental plot, but from a representative soil profile, and their representativeness in describing water infiltration and redistribution in different experimental plots seem to be important sources of error to consider. Soil hydraulic properties were determined in the laboratory on soil samples of a certain size (from 100 to 630 cm^3) and may not be representative of the much larger simulated flow domain under field conditions. For example, soil samples are normally saturated in the laboratory by capillarity, with water entering the sample through the bottom, decreasing the possibility of the air being trapped inside. For this reason, saturation values are usually much higher in the laboratory than under field conditions (Šimůnek et al., 1998), where this obviously cannot be accomplished. This may explain some of the deviations found in simulated water contents at a depth of 20 cm (Fig. 5) where HYDRUS-2D tended to simulate higher values during irrigation seasons than what field data showed. Additionally, the soil was considered homogeneous in HYDRUS-2D simulations, and more complex physical phenomena, such as spatial and temporal variability of the soil hydraulic properties and the probable existence of preferential flow paths in the different experimental plots, were neglected. Considering these additional phenomena in HYDRUS simulations would likely have helped improve the agreement between measured and simulated data.

It is also important for water flow simulations to accurately estimate plant transpiration and soil evaporation. The dual crop coefficient approach used is generally considered accurate (Tolk and Howell, 2001; Howell et al., 2004; Liu and Luo, 2010), but is complex and requires various crop and soil parameters that need to be adjusted to experimental conditions. Finally, the crop parameters, such as those used in the Feddes et al. (1978) model, were taken from the literature and do not take differences among crop varieties into account. The Maas (1990) threshold and slope parameters, which were mainly intended to serve as a guideline to relative tolerances among crops, may vary with cultivars, climate, soil conditions, and cultural practices. Thus, estimates of uptake reductions must be regarded with some uncertainty (Skaggs et al., 2006b). The same can be said about the empirical relationship between EC_e and EC_{sw}.

Model structure (or modeling approach) errors: Limitations involved in considering an axisymmetrical domain to represent the three-dimensional movement of water and nutrients have to be considered. This approach has been widely used for analyzing surface and buried drip irrigation experiments (Cote et al., 2003; Skaggs et al., 2004; Gärdenäs et al., 2005; Lazarovitch et al., 2005; Hanson et al., 2006; Ajdary et al., 2007; Kandelous and Šimůnek, 2010a,b; Ravikumar et al., 2011). Nevertheless, Kandelous et al. (2011) pointed out some of the limitations of this approach to be considered. Namely, the fact that flow from each emitter only remains axisymmetrical until the wetting patterns from neighboring emitters begin overlapping each other. Kandelous et al. (2011) state that the axisymmetrical representation is only an approximation of the fully three-dimensional problem and that the numerical results should increasingly depart from reality as time and irrigation volumes increase. Using a fully three-dimensional model, which is also available in HYDRUS (2D/3D), could improve water content simulations. In Ramos et al. (2011), a 1D version of HYDRUS, used for simulating a similar experiment, produced a RMSE (0.04 $cm^3\ cm^{-3}$) larger than the 2D approach (0.03 $cm^3\ cm^{-3}$) adapted in this study. Thus, adopting the 2D version of HYDRUS proved to be beneficial in lowering the simulation errors. However, numerical modeling is not that straightforward, and the notion that using a fully three-dimensional model would immediately bring better correspondence between measured and simulated data is unrealistic. The agreement between measured and simulated N—NO_3^- obtained here can serve as an example, since these results were worse than those obtained by Ramos et al. (2011). Considering a cylindrically shaped (0.375 m wide) simulation domain (Fig. 3) could be another possible model structure error, since the drip emitters' grid was in fact rectangular (0.75 m wide × 1 m long). This means that, in reality, water and solutes could redistribute in a larger soil domain than that considered in simulations.

Modeling of the N species: There are some additional considerations that need to be taken into account with regards to modeling the nitrogen fate and transport. The approach to model the transport of the nitrogen species using the sequential first-order decay chain reactions is relatively simple and has produced satisfactory results in many different studies (Ajdary et al., 2007; Mailhol et al., 2007; Crevoisier et al., 2008). However, this approach can only consider nitrogen processes that are involved in a sequential-first order decay chain, such as nitrification (N—NH_4^+ transformation into

$N—NO_2^-$, and then further into $N—NO_3^-$), denitrification ($N—NO_3^-$ transformation into N_2 and $N—N_2O$), and volatilization ($N—NH_4^+$ transformation into $N—NH_3$). Other nitrogen reactions, with probable relevance for long-term applications such as ours, simply cannot be accounted for using this approach. Examples of such reactions are nitrogen fixation from the atmosphere, mineralization of crop residues and other organic wastes, mineralization of the soil humus fraction, and so on. The relevance of these processes on N dynamics can be documented in Fig. 10, which shows that $N—NH_4^+$ and $N—NO_3^-$ concentrations in the soil increased after fertigation events during crop seasons, and then decreased due to plant uptake and leaching. During fertigation events, simulations matched the measured data well since nitrification was the main process occurring in the soil. However, the deviation between measured and simulated N data was visually more pronounced during non-crop seasons, due to the limitations discussed above. For example, sweet sorghum was harvested at the end of the growing season so that its biomass production could be estimated. This involved cutting the entire plant above the ground while leaving roots in the soil. Residual $N—NH_4^+$ and $N—NO_3^-$ concentrations measured during non-crop seasons could, to some extent, be attributed to the mineralization of the root system, and thus were not considered in model simulations.

Additionally, only the passive nutrient uptake mechanism was considered in our approach. Since root nitrogen uptake likely involves both passive and active mechanisms (e.g., Šimůnek and Hopmans, 2009), considering only passive uptake likely underestimated the total N uptake and overestimated downward N leaching, providing thus the most conservative assessment of N leaching. However, the extent of this underestimation is currently unknown. Finally, deviations between measured and simulated N data could also be attributed to other model limitations and relevant physical phenomena that were not considered in our modeling approach, such as root growth.

4. Conclusions

The irrigation scheme used in this study allowed investigation of the response of sweet sorghum to irrigation scenarios with different levels of nitrogen and different water qualities between 2007 and 2010. The water contents, EC_{sw}, $N—NH_4^+$ and $N—NO_3^-$ concentrations simulated continuously during the entire field experiment, compared well with collected experimental data, having a RMSE of 0.030 $cm^3\ cm^{-3}$, 1.764 $dS\ m^{-1}$, 0.042 $mmol_c\ L^{-1}$, and 3.078 $mmol_c\ L^{-1}$, respectively. Possible causes of deviations between measured data and simulations were likely related to field measurements, model input data, and model structure errors, and were extensively discussed, showing HYDRUS-2D advantages and limitations for this application. However, model simulations helped to understand the best irrigation and fertigation management practices to be adopted in order to increase nutrient uptake and reduce nutrient leaching.

Sweet sorghum transpiration was estimated to vary between 360 and 457 mm depending on the crop season and the irrigation scenario considered. The lower water needs of sweet sorghum, compared to other traditional crops grown in water-scarce European Mediterranean regions, make it a good alternative to other crops for these environmentally stressed regions.

Sweet sorghum appears to be tolerant to the use of saline waters. Only during the second crop season, but mainly during the 3rd year, started the sweet sorghum transpiration be reduced due to the increase in the salinity stress and salt accumulation over time. Thus, in water-scarce regions where even saline waters can be viewed as an important source of irrigation water during drought seasons, the use of marginal waters showed viability for irrigating sweet sorghum during a limited time period.

HYDRUS-2D successfully estimated the fate of nitrogen in field plots grown with sweet sorghum under European Mediterranean conditions. The logarithmic function describing the relation between estimates of $N—NO_3^-$ uptake and the dry biomass yield ($R^2 = 0.71$) showed that sweet sorghum N requirements were lower than estimated N uptakes for the scenario with the highest levels of applied nitrogen, revealing some luxury uptake in these plots. The leaching of N out of the root zone depended closely on drainage, the amount of N applied, the form of N in the fertilizer, and the time and number of fertigation events. Based on model simulations, leaching of nitrogen occurred mainly in the $N—NO_3^-$ form, reaching 41–70% of the total amount of $N—NO_3^-$ available in the soil system. According to HYDRUS-2D, higher $N—NO_3^-$ uptakes were obtained when the number of fertigation events was larger.

Acknowledgments

This work was funded by the Project PTDC/AGR-AAM/66004/2006 of the Fundação para a Ciência e a Tecnologia (FCT). T. B. Ramos was funded by the FCT grant SFRH/BD/60363/2009.

References

Ajdary, K., Singh, D.K., Singh, A.K., Khanna, M., 2007. Modelling of nitrogen leaching from experimental onion field under drip irrigation. Agricultural Water Management 89, 15–28.

Allen, R.G., Pereira, L.S., Raes, D., Smith, M., 1998. Crop evapotranspiration – guidelines for computing crop water requirements. Irrig. Drain. Pap. 56. FAO, Rome, Italy.

Allen, R.G., Pereira, L.S., Smith, M., Raes, D., Wright, J.L., 2005. FAO-56 dual crop coefficient method for estimating evaporation from soil and application extensions. Journal of Irrigation and Drainage Engineering 131, 2–13.

Almodares, A., Hadi, M.R., 2009. Production of bioethanol from sweet sorghum: a review. African Journal of Agricultural Research 4, 772–780.

Barbanti, L., Grandi, S., Vecchi, A., Venturi, G., 2006. Sweet and fibre sorghum (*Sorghum bicolor* (L.) Moench), energy crops in the frame of environmental protection from excessive nitrogen loads. European Journal of Agronomy 25, 30–39.

Bear, J., 1972. Dynamics of Fluids in Porous Media. Elsevier, New York.

Cameira, M.R., Fernando, R.M., Pereira, L.S., 2003. Monitoring water and NO_3—N in irrigated maize fields in the Sorraia Watershed, Portugal. Agricultural Water Management 60, 199–216.

Cameira, M.R., Fernando, R.M., Ahuja, L.R., Pereira, L.S., 2005. Simulating the fate of water in field soil–crop environment. Journal of Hydrology 315, 1–24.

Cameira, M.R., Fernando, R.M., Ahuja, L.R., Ma, L., 2007. Using RZWQM to simulate the fate of nitrogen in field soil–crop environment in the Mediterranean region. Agricultural Water Management 90, 121–136.

Cote, C.M., Bristow, K.L., Charlesworth, P.B., Cook, F.J., Thorburn, P.J., 2003. Analysis of soil wetting and solute transport in subsurface trickle irrigation. Irrigation Science 22, 143–156.

Crevoisier, D., Popova, Z., Mailhol, J.C., Ruelle, P., 2008. Assessment and simulation of water and nitrogen transfer under furrow irrigation. Agricultural Water Management 95, 354–366.

Doltra, J., Muñoz, P., 2010. Simulation of nitrogen leaching from a fertigated crop rotation in a Mediterranean climate using the EU-Rotate_N and Hydrus-2D models. Agricultural Water Management 97, 277–285.

European Commission, 2010a. On implementation of Council Directive 91/676/EEC concerning the protection of waters against pollution caused by nitrates from agricultural sources based on Member State reports for the period 2004–2007. Report from the Commission to the Council and the European Parliament 47, Brussels.

European Commission, 2010b. On implementation of Council Directive 91/676/EEC concerning the protection of waters against pollution caused by nitrates from agricultural sources based on Member State reports for the period 2004–2007. Accompanying document to the report from the Commission to the Council and the European Parliament. Commission Staff Working Document 118, Brussels.

FAO, 2006. World reference base for soil resources. A framework for international classification, correlation and communication. World soil resources reports 103. Food and Agriculture Organization of the United Nations, Rome.

Feddes, R.A., Kowalik, P.J., Zaradny, H., 1978. Simulation of field water use and crop yield. Simulation Monographs Pudoc. Wageningen, The Netherlands.

Fernando, R.M., 1993. Quantificação do balanço hídrico de um solo regado na presença de uma toalha freática. Simulação com o modelo SWATRER. PhD thesis. Institute of Agronomy, Technical University of Lisbon, Lisbon, Portugal.

Ferré, T.P.A., Nissen, H.H., Šimůnek, J., 2002. The effect of the spatial sensitivity of TDR on inferring soil hydraulic properties from water content measurements made during the advance of a wetting front. Vadose Zone Journal 1, 281–288.

Fontes, J.C., Pereira, L.S., Smith, R.E., 1992. Runoff and erosion in volcanic soils of Azores: simulation with OPUS. Catena 56, 199–212.
Gärdenäs, A., Hopmans, J.W., Hanson, B.R., Šimůnek, J., 2005. Two-dimensional modeling of nitrate leaching for various fertigation scenarios under micro-irrigation. Agricultural Water Management 74, 219–242.
Gonçalves, M.C., Leij, F.J., Schaap, M.G., 2001. Pedotransfer functions for solute transport parameters of Portuguese soils. European Journal of Soil Science 52, 563–574.
Gonçalves, M.C., Šimůnek, J., Ramos, T.B., Martins, J.C., Neves, M.J., Pires, F.P., 2006. Multicomponent solute transport in soil lysimeters with waters of different quality. Water Resources Research 42, W08401, http://dx.doi.org/10.1029/2005WR004802.
Hanson, B.R., Šimůnek, J., Hopmans, J.W., 2006. Evaluation of urea-ammonium-nitrate fertigation with drip irrigation using numerical modeling. Agricultural Water Management 86, 102–113.
Hanson, B.R., Šimůnek, J., Hopmans, J.W., 2008. Leaching with subsurface drip irrigation under saline, shallow ground water conditions. Vadose Zone Journal 7, 810–818.
Hoffman, G.J., Shalhevet, J., 2007. Controlling salinity. In: Hoffman, G.J. (Ed.), Design and operation of farm irrigation systems. , 2nd ed. American Society of Agricultural and Biological Engineers, St. Joseph, Michigan, USA, pp. 160–207.
Howell, T.A., Evett, R., Tolk, J.A., Schneider, A.D., 2004. Evapotranspiration of full-, deficit-irrigated, and dryland cotton on the Northern Texas High Plains. Journal of Irrigation and Drainage Engineering 130, 277–285.
Hutson, J.L., Wagenet, R.J., 1991. Simulating nitrogen dynamics in soils using a deterministic model. Soil Use and Management 7, 74–78.
Johnsson, H., Bergström, L., Jansson, P.-E., Paustian, K., 1987. Simulated nitrogen dynamics and losses in a layered agricultural soil. Agriculture Ecosystems and Environment 18, 333–356.
Kandelous, M.M., Šimůnek, J., 2010a. Comparison of numerical, analytical and empirical models to estimate wetting pattern for surface and subsurface drip irrigation. Irrigation Science 28, 435–444.
Kandelous, M.M., Šimůnek, J., 2010b. Numerical simulations of water movement in a subsurface drip irrigation system under field and laboratory conditions using HYDRUS-2D. Agricultural Water Management 97, 1070–1076.
Kandelous, M.M., Šimůnek, J., van Genuchten, M.Th., Malek, K., 2011. Soil water content distributions between two emitters of a subsurface drip irrigation system. Soil Science Society of America Journal 75, 488–497.
Katerji, N., Mastrorilli, M., Rana, G., 2008. Water use efficiency of crops cultivated in the Mediterranean region: review and analysis. European Journal of Agronomy 28, 493–507.
Klepper, B., 1991. Crop root system response to irrigation. Irrigation Science 12, 105–108.
Lazarovitch, N., Šimůnek, J., Shani, U., 2005. System-dependent boundary condition for water flow from subsurface source. Soil Science Society of America Journal 69, 46–50.
Liu, Y.J., Luo, Y., 2010. A consolidated evaluation of the FAO-56 dual crop coefficient approach using the lysimeter data in the North China Plain. Agricultural Water Management 97, 31–40.
Ma, L., Ahuja, L.R., Ascough II, J.C., Shaffer, M.J., Rojas, K.W., Malone, R.W., Cameira, M.R., 2001. Integrating system modeling with field research in agriculture: applications of the root zone water quality model (RZWQM). Advances in Agronomy 71, 233–292.
Mailhol, J.C., Crevoisier, D., Triki, K., 2007. Impact of water application conditions on nitrogen leaching under furrow irrigation: experimental and modelling approaches. Agricultural Water Management 87, 275–284.
Mailhol, J.C., Ruelle, P., Walser, S., Schütze, N., Dejean, C., 2011. Analysis of AET and yield predictions under surface and buried drip irrigation systems using the Crop Model PILOTE and Hydrus-2D. Agricultural Water Management 98, 1033–1044.
Mallants, D., van Genuchten, M.Th., Šimůnek, J., Jacques, D., Seetharam, S., 2011. Leaching of contaminants to groundwater. In: Swartjes, F.A. (Ed.), Dealing with Contaminated Sites. From Theory to Practical Applications. Springer, The Netherlands, pp. 787–850.
Maas, E.V., 1990. Crop salt tolerance. In: Tanji, K.K. (Ed.), Agricultural Salinity Assessment and Management. Manual on Engineering Practice, vol. 71. American Society of Civil Engineers, Reston, VA, pp. 262–304.
Mastrorilli, M., Katerji, N., Rana, G., Steduto, P., 1995. Sweet sorghum in Mediterranean climate: radiation use and biomass water use efficiencies. Industrial Crop and Products 3, 253–260.
Mastrorilli, M., Katerji, N., Rana, G., 1999. Productivity and water use efficiency of sweet sorghum as affected by soil water deficit occurring at different vegetative growth stages. European Journal of Agronomy 11, 207–215.
Mmolawa, K., Or, D., 2003. Experimental and numerical evaluation of analytical volume balance model for soil water dynamics under drip irrigation. Soil Science Society of America Journal 67, 1657–1671.
Novák, V., van Genuchten, M.Th., 2008. Using the transpiration regime to estimate biomass production. Soil Science 173, 401–407.
Pereira, L.S., van den Broek, B., Kabat, P., Allen, R.G., 1995. Crop–Water Simulation Models in Practice. Wageningen Pers, Wageningen, The Netherlands.
Prasad, S., Singh, A., Jain, N., Joshi, H.C., 2007. Ethanol production from sweet sorghum syrup for utilization as automotive fuel in India. Energy and Fuel 21, 2415–2420.
Ramos, T.B., Gonçalves, M.C., Castanheira, N.L., Martins, J.C., Santos, F.L., Prazeres, A., Fernandes, M.L., 2009. Effect of sodium and nitrogen on yield function of irrigated maize in southern Portugal. Agricultural Water Management 96, 585–594.
Ramos, T.B., Šimůnek, J., Gonçalves, M.C., Martins, J.C., Prazeres, A., Castanheira, N.L., Pereira, L.S., 2011. Field evaluation of a multicomponent solute transport model in soils irrigated with saline waters. Journal of Hydrology 407, 129–144, http://dx.doi.org/10.1016/j.jhydrol.2011.07.016.
Ramos, T.B., Castanheira, N.L., Gonçalves, M.C., Fernandes, M.L., Januário, M.I., Lourenço, M.E., Pires, F.P., Martins, J.C., 2012. Effect of combined use of brackish water and nitrogen fertilizer on biomass and sugar yield of sweet sorghum. Pedosphere, in press.
Ravikumar, V., Vijayakumar, G., Šimůnek, J., Chellamuthu, S., Santhi, R., Appavu, K., 2011. Evaluation of fertigation scheduling for sugarcane using a vadose zone flow and transport model. Agricultural Water Management 98, 1431–1440.
Ritchie, J.T., 1972. Model for predicting evaporation from a row crop with incomplete cover. Water Resources Research 8, 1204–1213.
Roberts, T., Lazarovitch, N., Warrick, A.W., Thompson, T.L., 2009. Modeling salt accumulation with subsurface drip irrigation using HYDRUS-2D. Soil Science Society of America Journal 73, 233–240.
Roberts, T., White, S.A., Warrick, A.W., Thompson, T.L., 2008. Tape depth and germination method influence patterns of salt accumulation with subsurface drip irrigation. Agricultural Water Management 95, 669–677.
Rosa, R.D., Paredes, P., Rodrigues, G.C., Alves, I., Fernando, R.M., Pereira, L.S., Allen, R.G., 2012. Implementing the dual crop coefficient approach in interactive software: 1. Background and computational strategy. Agricultural Water Management 103, 62–77.
Šimůnek, J., Wang, D., Shouse, P.J., van Genuchten, Th.M., 1998. Analysis of a field tension disc infiltrometer experiment by parameter estimation. International Agrophysics 12, 167–180.
Šimůnek, J., van Genuchten, Th.M., Šejna, M., 2006. The HYDRUS software package for simulating two- and three-dimensional movement of water, heat, and multiple solutes in variably-saturated media. In: Technical Manual. Version 1.0. PC Progress, Prague, Czech Republic, 241 p.
Šimůnek, J., van Genuchten, M.Th., Šejna, M., 2008. Development and applications of the HYDRUS and STANMOD software packages, and related codes. Vadose Zone Journal 7, 587–600.
Šimůnek, J., Hopmans, J.W., 2009. Modeling compensated root water and nutrient uptake. Ecological Modelling 220, 505–521.
Skaggs, T.H., Trout, T.J., Šimůnek, J., Shouse, P.J., 2004. Comparison of HYDRUS-2D simulations of drip irrigation with experimental observations. Journal of Irrigation and Drainage Engineering 130, 304–310.
Skaggs, T.H., van Genuchten M.Th. Shouse, P.J., Poss, J.A., 2006a. Macroscopic approaches to root water uptake as a function of water and salinity stress. Agricultural Water Management 86, 140–149.
Skaggs, T.H., Shouse, P.J., Poss, J.A., 2006b. Irrigating forage crops with saline waters: 2. Modeling root uptake and drainage. Vadose Zone Journal 5, 824–837.
Steduto, P., Katerji, N., Puertos-Molina, H., Unlü, M., Mastrorilli, M., Rana, G., 1997. Water-use efficiency of sweet sorghum under water stress conditions. Gas-exchange investigations at leaf and canopy scales. Field Crops Research 54, 221–234.
Tolk, J.A., Howell, T.A., 2001. Measured and simulated evapotranspiration of grain sorghum grown with full and limited irrigation in three High Plains soils. Transactions of ASABE 44, 1553–1558.
U.S. Salinity Laboratory Staff, 1954. Diagnosis and Improvement of Saline and Alcaly Soils. USDA Handbook 60. Washington, USA.
van Genuchten, M.Th., 1980. A closed form equation for predicting the hydraulic conductivity of unsaturated soils. Soil Science Society of America Journal 44, 892–898.
van Genuchten, M.Th., 1987. A numerical model for water and solute movement in and below the root zone. Res. Rep. 121, U.S. Salinity Laboratory, USDA, ARS, Riverside, California.
Vasilakoglou, I., Dhima, K., Karagiannidis, N., Gatsis, T., 2011. Sweet sorghum productivity for biofuels under increased soil salinity and reduced irrigation. Field Crops Research 120, 38–46.
Vrugt, J.A., Hopmans, J.W., Šimůnek, J., 2001. Calibration of a two dimensional root water uptake model. Soil Science Society of America Journal 65, 1027–1037.
Weihermüller, L., Kasteel, R., Vanderborght, J., Pütz, T., Vereecken, H., 2005. Soil water extraction with a suction cup: results of numerical simulations. Vadose Zone Journal 4, 899–907.
Weihermüller, L., Kasteel, R., Vanderborght, J., Šimůnek, J., Vereecken, H., 2011. Uncertainty in pesticide monitoring using suction cups: evidence from numerical simulations. Vadose Zone Journal 10, 1287–1298.
Zegada-Lizarazu, W., Zatta, A., Monti, A., 2012. Water uptake efficiency and above- and belowground biomass development of sweet sorghum and maize under different water regimes. Plant Soil 351, 47–60.
Zhao, Y.L., Dolat, A., Steinberger, Y., Wang, X., Osman, A., Xie, G.H., 2009. Biomass yield and changes in chemical composition of sweet sorghum cultivars grown for biofuel. Field Crops Research 111, 55–64.